

Doubled Color Codes

Sergey Bravyi* Andrew Cross*

Abstract

We show how to perform a fault-tolerant universal quantum computation in 2D architectures using only transversal unitary operators and local syndrome measurements. Our approach is based on a doubled version of the 2D color code. It enables a transversal implementation of all logical gates in the Clifford+ T basis using the gauge fixing method proposed recently by Paetznick and Reichardt. The gauge fixing requires six-qubit parity measurements for Pauli operators supported on faces of the honeycomb lattice with two qubits per site. Doubled color codes are promising candidates for the experimental demonstration of logical gates since they do not require state distillation. Secondly, we propose a Maximum Likelihood algorithm for the error correction and gauge fixing tasks that enables a numerical simulation of logical circuits in the Clifford+ T basis. The algorithm can be used in the online regime such that a new error syndrome is revealed at each time step. We estimate the average number of logical gates that can be implemented reliably for the smallest doubled color code and a toy noise model that includes depolarizing memory errors and syndrome measurement errors.

*IBM T.J. Watson Research Center, Yorktown Heights, NY 10598, USA

Contents

1	Introduction	3
2	Notations	6
3	Subsystem quantum codes and gauge fixing	8
4	Transversal logical gates	10
5	Commuting Pauli errors through T -gates	12
6	Maximum likelihood error correction and gauge fixing	15
7	Logical Clifford+ T circuits with the 15-qubit code	22
8	Doubled color codes: main properties	28
9	Regular color codes	29
10	Doubling transformation	32
11	Doubled color codes: construction	34
12	Weight reduction	39

1 Introduction

Recent years have witnessed several major steps towards experimental demonstration of quantum error correction [1, 2, 3] giving us hope that a small-scale fault tolerant quantum memory may become a reality soon. Quantum memories based on topological stabilizer codes such as the 2D surface code are arguably among the most promising candidates since they can tolerate a high level of noise and can be realized on a two-dimensional grid of qubits with local parity checks [4, 5, 6]. Logical qubits encoded by such codes would be virtually isolated from the environment by means of an active error correction and could preserve delicate superpositions of quantum states for extended periods of time.

Meanwhile, demonstration of a universal set of logical gates required for a fault-tolerant quantum computing remains a distant goal. Although the surface code provides a low-overhead implementation of logical Clifford gates such as the CNOT or the Hadamard gate [5, 6], implementation of logical non-Clifford gates poses a serious challenge. Non-Clifford gates such as the single-qubit 45° phase shift known as the T -gate are required to express interesting quantum algorithms but their operational cost in the surface code architecture exceeds the one of Clifford gates by orders of magnitude. This large overhead stems from the state distillation subroutines which may require a thousand or more physical qubits to realize just a single logical T -gate [7, 8]. Some form of state distillation is used by all currently known fault-tolerant protocols based on 2D stabilizer codes.

The purpose of this paper is to propose an alternative family of quantum codes and fault tolerant protocols for 2D architectures where all logical gates are implemented transversally. Recall that a logical gate is called transversal if it can be implemented by applying some single-qubit rotations to each physical qubit. Transversal gates are highly desirable since they introduce no overhead and do not spread errors. Assuming that all qubits are controlled in parallel, a transversal gate takes the same time as a single-qubit rotation, which is arguably the best one can hope for. Unfortunately, transversal gates have a very limited computational power. A no-go theorem proved by Eastin and Knill [9] asserts that a quantum code can have only a finite number of transversal gates which rules out universality. In the special case of 2D stabilizer codes a more restrictive version of this theorem have been proved asserting that transversal logical gates must belong to the Clifford group [10, 11, 12].

To circumvent these no-go theorems we employ the gauge fixing method proposed recently by Paetznick and Reichardt [13]. A fault-tolerant protocol based on the gauge fixing method alternates between two error correcting codes that provide a transversal implementation of logical Clifford gates and the logical T -gate respectively. Thus a computational universality is achieved by combining transversal gates of two different codes. A conversion between the codes can be made fault-tolerantly if their stabilizer groups have a sufficiently large intersection. This is achieved by properly choosing a pattern of parity checks measured at each time step and applying a gauge fixing operator depending on the measured syndromes. The latter is responsible both for error correction and for switching between two different encodings of the logical qubit.

Our goal for the first part of the paper (sections 3-7) is to develop effective error models and decoding algorithms suitable for simulation of logical circuits in the Clifford+ T basis. Although a transversal implementation of logical T -gates offers a substantial overhead reduction, it poses several challenges for the decoding algorithm. First, T -gates introduce correlations between X -type and

Z -type errors that cannot be described by the standard stabilizer formalism. This may prevent the decoder from using error syndromes measured before application of a T -gate in the error correction steps performed afterwards. Second, implementation of T -gates by the gauge fixing method requires an online decoder such that a new gauge fixing operator has to be computed and applied prior to each logical T -gate. Thus a practical decoder must have running time $O(1)$ per logical gate independent of the total length of the circuit. The present work makes two contributions that partially address these challenges.

First, we generalize the stabilizer formalism commonly used for a numerical simulation of error correction to logical Clifford+ T circuits. Specifically, we show how to commute Pauli errors through a composition of a transversal T -gate and a certain twirling map such that the effective error model at each step of the circuit can be described by random Pauli errors, even though the circuit may contain many non-Clifford gates. The twirling map has no effect on the logical state since it includes only stabilizer operators. We expect that this technique may find applications in other contexts.

Second, we propose a Maximum Likelihood (ML) decoding algorithm for the error correction and gauge fixing tasks. The ML decoder applies the Bayes rule to find a recovery operator which is most likely to succeed in a given task based on the full history of measured syndromes. This is achieved by properly taking into account statistics of memory and measurement errors, as well as correlations between X -type and Z -type errors introduced by transversal T -gates. Although the number of syndromes that the ML decoder has to process scales linearly with the length of the logical circuit, the decoder has a constant running time per logical gate which scales as $O(n2^n)$ for a code with n physical qubits. The decoder can be used in the online regime for sufficiently small codes, which is crucial for the future experimental demonstration of logical gates. A key ingredient of the decoder is the fast Walsh-Hadamard transform. A heuristic approximate version of the algorithm called a sparse ML decoder is proposed that could be applicable to medium size codes.

We apply the ML decoder to a particular gauge fixing protocol proposed by Anderson et al [14]. The protocol alternates between the 15-qubit Reed-Muller code and the 7-qubit Steane code that provide a transversal implementation of the T -gate and Clifford gates respectively. Numerical simulations are performed for a phenomenological error model that consists of depolarizing memory errors and syndrome measurement errors with some rate p . Following ideas of a randomized benchmarking [15, 16] we choose a Clifford+ T circuit at random, such that each Clifford gate is drawn from the uniform distribution on the single-qubit Clifford group. The circuit alternates between Clifford and T gates. The quantity we are interested in is a logical error rate defined as $p_L = 1/g$, where g is the average number of logical gates implemented before the first failure in the error correction or gauge fixing subroutines. Here g includes both Clifford and T gates. The sparse ML decoder enables a numerical simulation of circuits with more than 10,000 logical gates. For small error rates we observed a scaling $p_L = Cp^2$ with $C \approx 182$. Assuming that a physical Clifford+ T circuit has an error probability p per gate, the logical circuit becomes more reliable than the physical one provided that $p_L < p$, that is, $p < p_0 = C^{-1} \approx 0.55\%$. This value can be viewed as an “error threshold” of the proposed protocol. The observed threshold is comparable with the one calculated by Brown et al [17] for a gauge fixing protocol based on the 3D color codes which were recently proposed by Bombin [18]. We note however that Ref. [17] studied only the storage of a logical qubit (no logical

gates). We anticipate that the tools developed in the present paper could be used to simulate logical Clifford+ T circuits based on the 3D color codes as well. It should be pointed out that the threshold $p_0 = 0.55\%$ is almost one order of magnitude smaller than the one of the 2D surface code for the analogous error model [19]. This is the price one has to pay for the low-overhead implementation of all logical gates.

The numerical results obtained for the 15-qubit code call for more general code constructions that could achieve a more favorable scaling of the logical error rate. In the second part of the paper (sections 8-12) we propose an infinite family of 2D quantum codes with a diverging code distance that enable implementation of Clifford+ T circuits by the gauge fixing method. The number of physical qubits required to achieve a code distance $d = 2t + 1$ is $n = 2t^3 + 8t^2 + 6t - 1$. For comparison, the 3D color codes of Ref. [18] require $n = 4t^3 + 6t^2 + 4t + 1$ physical qubits. The new codes can be embedded into the 2D honeycomb lattice with two qubits per site such that all syndrome measurements required for error correction and gauge fixing are spatially local. More precisely, any check operator measured in the protocol acts on at most six qubits located on some face of the lattice. As was pointed out in Ref. [18], the gauge fixing method circumvents no-go theorems proved for transversal non-Clifford gates in the 2D geometry [10, 11, 12] since the decoder that controls all quantum operation may perform a non-local classical processing.

The key ingredient of our approach is a doubling transformation from the classical coding theory originally proposed by Betsumiya and Munemasa [20]. Its quantum analogue can be used to construct high-distance codes with a special symmetry required for transversality of logical T -gates. Namely, a quantum code of CSS type [21, 22] is said to be triply even (doubly even) if the weight of any X -type stabilizer is a multiple of eight (multiple of four). Any triply even CSS code of odd length is known to have a transversal T -gate. The doubling transformation combines a triply even code with distance $d - 2$ and two copies of a doubly even code with distance d to produce a triply even code with distance d . Our construction recursively applies the doubling transformation to the family of regular color codes on the honeycomb lattice [23] such that each recursion level increases the code distance by two. The regular color codes are known to be doubly even [24] (in a certain generalized sense). Producing a distance- d triply even code requires $(d - 1)/2$ recursion levels that combine color codes with distance $3, 5, \dots, d$. We refer to the new family of codes as doubled color code since the construction relies on taking two copies of the regular color codes. It should not be confused with the quantum double construction from the topological quantum field theory [25]. Doubled color codes have almost all properties required for implementation of logical Clifford+ T circuits by the gauge fixing method. Namely, a doubled color code has a transversal T -gate and can be converted fault-tolerantly to the regular color code which is known to have transversal Clifford gates [24]. Unfortunately, the doubling transformation does not preserve spatial locality of check operators. Even worse, some check operators of a doubled color code have very large weight and their syndromes cannot be measured in a fault-tolerant fashion. Converting the doubled color codes into a local form is our main technical contribution. This is achieved in two steps. First we show how to implement all levels of the recursive doubling transformation on the honeycomb lattice with two qubits per site such that almost all check operators of the output code are spatially local. We show that each of the remaining non-local checks can be decomposed into a product of local ones

by introducing several ancillary qubits and extending the code properly to the ancillary qubits. This technique is reminiscent of perturbation theory gadgets that are used to generate effective low-energy Hamiltonians with long-range many-body interactions starting from a simpler high-energy Hamiltonian with short-range two-body interactions [26].

The 15-qubit code studied in Section 7 can be viewed as the smallest example of a doubled color code. Furthermore, the 49-qubit triply even code with distance $d = 5$ discovered by an exhaustive numerical search in Ref. [27] can be viewed as a doubled color code obtained from the regular color code $[[17, 1, 5]]$ on the square-octagon lattice via the doubling transformation. The 49-qubit code is optimal in the sense that no distance-5 code with less than 49 qubits can be triply even [20, 27]. Thus the family of doubled color codes includes the best known examples of triply even codes with a small distance.

Although this paper focuses on codes with a single logical qubit, our fault-tolerant protocols can be incorporated into the lattice surgery method based on the regular color codes [28]. The former would provide implementation of logical single-qubit rotations decomposed into a product of Clifford and T -gates while the latter enables logical CNOTs and can serve as a quantum memory. We note that efficient and nearly optimal algorithms for decomposing single-qubit rotations into a product of Clifford and T -gates have been proposed recently [29, 30].

To make the paper self-contained, we provide all necessary background on quantum codes of CSS type, the gauge fixing method, and transversal logical gates in Sections 2-4. The effective error model describing the action of transversal T -gates on random Pauli errors is developed in Section 5. We describe the ML decoding algorithm suitable for simulation of Clifford+ T circuits in Section 6. Numerical simulation of random Clifford+ T logical circuits based on the family of 15-qubit codes is described in Section 7. This section also serves as an example illustrating the general construction of doubled color codes. The latter is described in Sections 8-12. First, we highlight main properties of the doubled color codes in Section 8. Definition of regular 2D color codes and their properties are summarized in Section 9. Doubled color codes and their embedding into the honeycomb lattice are defined in Sections 10,11. The most technical part of the paper is Section 12 explaining how to convert doubled color codes into a spatially local form.

2 Notations

Let \mathbb{F}_2^n be the n -dimensional linear space over the binary field \mathbb{F}_2 . A vector $x \in \mathbb{F}_2^n$ is regarded as a column vector with components x_1, \dots, x_n . We shall write x^\top for the corresponding row vector. The set of integers $\{1, 2, \dots, n\}$ will be denoted $[n]$. Let $\text{supp}(x) \subseteq [n]$ be the support of x , that is, the subset of indexes i such that $x_i = 1$. We shall often identify a vector x and the subset $\text{supp}(x)$. Let $|x| \equiv |\text{supp}(x)|$ be the weight of x , that is, the number of non-zero components. Given a subset $A \subseteq [n]$ let $x_A \in \mathbb{F}_2^{|A|}$ be a restriction of x onto A , that is, a vector obtained from x by deleting all components x_i with $i \notin A$. Conversely, given a vector $y \in \mathbb{F}_2^{|A|}$ let $y[A] \in \mathbb{F}_2^n$ be a vector obtained from y by inserting zero components for all $i \notin A$. For example, if $n = 5$, $A = \{1, 3, 5\}$, and $y = (111)$ then $y[A] = (10101)$. The space \mathbb{F}_2^n is equipped with a standard basis e^1, e^2, \dots, e^n , where $e^j \equiv 1[j]$

is the vector with a single non-zero component indexed by j . We shall use notations $\bar{0}$ and $\bar{1}$ for the all-zeros and the all-ones vectors. The inner product between vectors $x, y \in \mathbb{F}_2^n$ is defined as

$$x^\top y = \sum_{i=1}^n x_i y_i \pmod{2}.$$

A linear subspace spanned by vectors $x^1, \dots, x^m \in \mathbb{F}_2^n$ will be denoted $\langle x^1, \dots, x^m \rangle$. Given a subset $A \subseteq [n]$ and a subspace $\mathcal{S} \subseteq \mathbb{F}_2^{|A|}$, let $\mathcal{S}[A] \subseteq \mathbb{F}_2^n$ be the subspace spanned by vectors $y[A]$ with $y \in \mathcal{S}$. Let \mathcal{E}^n and \mathcal{O}^n be the subspaces of \mathbb{F}_2^n spanned by all even-weight and all odd-weight vectors respectively. We shall use shorthand notations $\mathcal{E} \equiv \mathcal{E}^n$ and $\mathcal{O} \equiv \mathcal{O}^n$ whenever the value of n is clear from the context. Given a linear subspace $\mathcal{S} \subseteq \mathbb{F}_2^n$ let \mathcal{S}^\perp be the orthogonal subspace,

$$\mathcal{S}^\perp = \{x \in \mathbb{F}_2^n : x^\top y = 0 \text{ for all } y \in \mathcal{S}\}$$

and $\dot{\mathcal{S}}$ be the subspace spanned by all even-weight vectors orthogonal to \mathcal{S} ,

$$\dot{\mathcal{S}} = \mathcal{S}^\perp \cap \mathcal{E}.$$

A subspace \mathcal{S} is self-orthogonal if $\mathcal{S} \subseteq \mathcal{S}^\perp$. We shall use identities $(\mathcal{S}^\perp)^\perp = \mathcal{S}$, $(\mathcal{S} + \mathcal{T})^\perp = \mathcal{S}^\perp \cap \mathcal{T}^\perp$, and $\mathcal{E}^\perp = \langle \bar{1} \rangle$. Given a subspace \mathcal{S} , let $d(\mathcal{S})$ be the minimum weight of odd-weight vectors in \mathcal{S}^\perp ,

$$d(\mathcal{S}) \equiv \min \{|f| : f \in \mathcal{S}^\perp \cap \mathcal{O}\}. \quad (1)$$

Consider now a system of n qubits and let X_j, Y_j, Z_j be the Pauli operators acting on a qubit j tensored with the identity on the remaining qubits. Given a vector $f \in \mathbb{F}_2^n$ and a single-qubit Pauli operator P let $P(f)$ be the n -qubit operator that applies P to each qubit in the support of f ,

$$P(f) = \prod_{j \in \text{supp}(f)} P_j.$$

For any subset $\mathcal{S} \subseteq \mathbb{F}_2^n$ define the corresponding set of Pauli operators $P(\mathcal{S}) \equiv \{P(f) : f \in \mathcal{S}\}$. A pair of subspaces $\mathcal{A}, \mathcal{B} \subseteq \mathbb{F}_2^n$ defines a group of n -qubit Pauli operators

$$\text{CSS}(\mathcal{A}, \mathcal{B}) = \langle X(\mathcal{A}), Z(\mathcal{B}) \rangle.$$

Any element of $\text{CSS}(\mathcal{A}, \mathcal{B})$ has a form $i^m X(f)Z(g)$ for some $f \in \mathcal{A}$, $g \in \mathcal{B}$, and some integer m . Note that the group $\text{CSS}(\mathcal{A}, \mathcal{B})$ is abelian iff \mathcal{A} and \mathcal{B} are mutually orthogonal, $\mathcal{A} \subseteq \mathcal{B}^\perp$, since

$$X(f)Z(g) = (-1)^{f^\top g} Z(g)X(f).$$

Given a vector $f \in \mathbb{F}_2^n$, let $|f\rangle = |f_1 \otimes \dots \otimes f_n\rangle$ be the corresponding basis state of n qubits. Note that $|f\rangle = X(f)|\bar{0}\rangle$.

3 Subsystem quantum codes and gauge fixing

This section summarizes some known facts concerning subsystem quantum codes of Calderbank-Steane-Shor (CSS) type [21, 22] and the gauge fixing method. A quantum CSS code is constructed from a pair of linear subspaces $\mathcal{A}, \mathcal{B} \subseteq \mathbb{F}_2^n$ that are mutually orthogonal, $\mathcal{A} \subseteq \mathcal{B}^\perp$. Such pair defines an abelian group of Pauli operators $\mathcal{S} = \text{CSS}(\mathcal{A}, \mathcal{B})$ called a *stabilizer group*. Elements of \mathcal{S} are called stabilizers. We shall often identify a CSS code and its stabilizer group. A subspace spanned by n -qubit states invariant under the action of any stabilizer is called a *codespace*. A projector onto the codespace can be written as

$$\Pi = \frac{1}{|\mathcal{S}|} \sum_{G \in \mathcal{S}} G. \quad (2)$$

In this paper we only consider a restricted class of CSS codes such that all vectors in \mathcal{A} and \mathcal{B} have even weight whereas the number of physical qubits n is odd,

$$n = 1 \pmod{2}, \quad \mathcal{A} \subseteq \mathcal{E}, \quad \mathcal{B} \subseteq \mathcal{E}. \quad (3)$$

We shall only consider codes with a single logical (encoded) qubit. Operators acting on the encoded qubit are expressed in terms of *logical Pauli operators*

$$X_L = X(\bar{1}), \quad Y_L = Y(\bar{1}), \quad Z_L = Z(\bar{1}). \quad (4)$$

Logical operators commute with any stabilizer due to Eq. (3) and thus preserve the codespace. Furthermore, X_L, Y_L, Z_L obey the same commutation rules as single-qubit Pauli operators X, Y, Z respectively. More generally, a Pauli operator P is called a logical operator iff it coincides with X_L, Y_L , or Z_L modulo stabilizers, that is, $P = X(a)Z(b)$, where $a \in \mathcal{A} + \alpha\bar{1}$, $b \in \mathcal{B} + \beta\bar{1}$, and at least one of the coefficients α, β is non-zero. A logical state encoding a single-qubit state $\eta = (1/2)(I + \alpha X + \beta Y + \gamma Z)$ is defined as

$$\rho_L \equiv \rho_L(\eta) = O_L \Pi, \quad O_L = \delta(I + \alpha X_L + \beta Y_L + \gamma Z_L), \quad (5)$$

where δ is a coefficient responsible for normalization $\text{Tr}(\rho_L) = 1$.

Pauli operators that commute with both stabilizers and logical operators generate a group \mathcal{G} called a *gauge group*. Elements of \mathcal{G} are called gauge operators. Note that a Pauli operator $X(f)$ commutes with all stabilizers iff $f \in \mathcal{B}^\perp$. Likewise, $X(f)$ commutes with the logical operators iff $\bar{1}^\top f = 0$, that is, $f \in \mathcal{E}$. Thus $X(f)$ is a gauge operator iff $f \in \dot{\mathcal{B}}$, where we use notations of Section 2. The same reasoning shows that $Z(g)$ is a gauge operator iff $g \in \dot{\mathcal{A}}$. Thus the gauge group corresponding to a stabilizer group $\mathcal{S} = \text{CSS}(\mathcal{A}, \mathcal{B})$ is given by

$$\mathcal{G} = \text{CSS}(\dot{\mathcal{B}}, \dot{\mathcal{A}}). \quad (6)$$

By definition, $\mathcal{S} \subseteq \mathcal{G}$. Note that $E \rho_L E^\dagger = \rho_L$ for any $E \in \mathcal{G}$, that is, gauge operators have no effect on the logical state.

A noise maps the logical state ρ_L to a probabilistic mixture of states $E_\alpha \rho_L E_\alpha^\dagger$, where E_α are some n -qubit Pauli operators called *memory errors* or simply errors. We shall only consider noise that

can be described by random Pauli errors. Note that errors E_α and E_β have the same action on any logical state whenever $E_\beta^\dagger E_\alpha \in \mathcal{G}$, that is, gauge-equivalent errors can be identified. We shall say that an error E is *non-trivial* if $E \notin \mathcal{G}$. Errors are diagnosed by measuring eigenvalues of some stabilizers. An eigenvalue measurement of a stabilizer $X(f)$ has an outcome $(-1)^{\xi(f)}$, where $\xi(f) \in \mathbb{F}_2$ is called a *syndrome* of $X(f)$. A corrupted state $E\rho_L E^\dagger$ with a memory error $E = X(a)Z(b)$ has a syndrome $\xi(f) = f^\top b$. It reveals whether E commutes or anti-commutes with $X(f)$. A syndrome of a stabilizer $Z(g)$ is defined as $\zeta(g) = g^\top a$. It reveals whether E commutes or anti-commutes with $Z(g)$. By definition, gauge-equivalent errors have the same syndromes.

In some cases stabilizer syndromes cannot be measured directly (for example, if a stabilizer has too large weight) but they can be inferred by measuring eigenvalues of some gauge operators. For example, suppose a stabilizer $X(f)$ can be represented as a product of X -type gauge operators $X(g^\alpha)$, that is, $f = g^1 + g^2 + \dots + g^m$ for some $f \in \mathcal{A}$ and $g^\alpha \in \dot{\mathcal{B}}$. An eigenvalue measurement of the gauge operator $X(g^\alpha)$ has an outcome $(-1)^{\xi(g^\alpha)}$, where $\xi(g^\alpha)$ is called a *gauge syndrome*. Once all gauge syndromes $\xi(g^\alpha)$ have been measured, the syndrome of $X(f)$ is inferred from $\xi(f) = \xi(g^1) + \dots + \xi(g^m)$. Since gauge operators commute with stabilizers, these measurements do not affect syndromes of any Z -type stabilizers. However, measuring gauge syndromes may change the encoded state and the latter no longer has a form $E_\alpha \rho_L E_\alpha^\dagger$ (since some gauge degrees of freedom have been fixed). We shall assume that each syndrome measurement is followed by a twirling map

$$\mathcal{W}_{\mathcal{G}}(\rho) = \frac{1}{|\mathcal{G}|} \sum_{G \in \mathcal{G}} G \rho G^\dagger$$

that applies a random gauge operator G drawn from the uniform distribution on \mathcal{G} . The twirling map restores the original form of the encoded state $E_\alpha \rho_L E_\alpha^\dagger$ by bringing all gauge degrees of freedom to the maximally mixed state. Gauge syndromes $\zeta(g^\alpha)$ for Z -type gauge operators $g^\alpha \in \dot{\mathcal{A}}$ are defined analogously.

A memory error E is said to be *undetectable* if it commutes with any element of \mathcal{S} . Equivalently, E has zero syndrome for any stabilizer. Errors E that are both undetectable and non-trivial ($E \notin \mathcal{G}$) should be avoided since they can alter the logical state. A *code distance* d is defined as the minimum weight of an undetectable non-trivial error. The code $\text{CSS}(\mathcal{A}, \mathcal{B})$ has distance

$$d = \min \{d(\mathcal{A}), d(\mathcal{B})\}, \quad (7)$$

where $d(\mathcal{A})$ and $d(\mathcal{B})$ are defined by Eq. (1).

Next let us discuss a *gauge fixing* operation that extends the stabilizer group to a larger group or, equivalently, reduces the gauge group to a smaller subgroup. Consider a pair of codes with stabilizer groups $\mathcal{S} = \text{CSS}(\mathcal{A}, \mathcal{B})$ and $\mathcal{S}' = \text{CSS}(\mathcal{A}', \mathcal{B}')$ such that $\mathcal{A} \subseteq \mathcal{A}'$ and $\mathcal{B} \subseteq \mathcal{B}'$. Let $\mathcal{G} = \text{CSS}(\dot{\mathcal{B}}, \dot{\mathcal{A}})$ and $\mathcal{G}' = \text{CSS}(\dot{\mathcal{B}}', \dot{\mathcal{A}}')$ be the respective gauge groups. We note that $\mathcal{S} \subseteq \mathcal{S}'$ and $\mathcal{G} \supseteq \mathcal{G}'$. Let us represent \mathcal{G} as a disjoint union of cosets $G_a \mathcal{G}'$ for some fixed set of coset representatives $G_1, \dots, G_m \in \mathcal{G}$. Simple algebra shows that the codespace projectors Π and Π' of the two codes are related as

$$\Pi = \sum_{a=1}^m G_a \Pi' G_a^\dagger, \quad (8)$$

and all subspaces $G_a \Pi' G_a^\dagger$ are pairwise orthogonal. Substituting Eq. (8) into Eq. (5) shows that any logical state ρ_L of the code \mathcal{S} can be written as

$$\rho_L = \frac{1}{m} \sum_{a=1}^m G_a \rho'_L G_a^\dagger, \quad (9)$$

where ρ'_L is a logical state of the code \mathcal{S}' . Furthermore, ρ_L and ρ'_L encode the same state. Since G_a are not gauge operators for the code \mathcal{S}' , they should be treated as memory errors. Moreover, any pair of errors G_a and G_b can be distinguished by measuring a complete syndrome of the code \mathcal{S}' (that is, measuring syndromes of some complete set of generators of \mathcal{S}'). Indeed, if G_a and G_b would have the same syndromes for some $a \neq b$ then the operator $G_a G_b^\dagger$ would commute with any element of \mathcal{S}' as well as with the logical operators. This would imply $G_a G_b^\dagger \in \mathcal{G}'$ which is a contradiction since $G_a \mathcal{G}' \neq G_b \mathcal{G}'$. Thus a complete syndrome measurement for the code \mathcal{S}' projects the state ρ_L in Eq. (9) onto some particular term $G_a \rho'_L G_a^\dagger$ and the coset $G_a \mathcal{G}'$ can be inferred from the measured syndrome. Applying a recovery operator R chosen as any representative of the coset $G_a \mathcal{G}'$ yields a state $R G_a \rho'_L G_a^\dagger R^\dagger = \rho'_L$. This completes the gauge fixing operation. The gauge fixing can be performed in the reverse direction as well. Namely, the encoded state ρ'_L can be mapped to ρ_L by applying randomly one of the operator G_1, \dots, G_m drawn from the uniform distribution, see Eq. (9). We shall collectively refer to the gauge fixing and its reverse as *code deformations*.

It will be convenient to distinguish between *subsystem* and *regular* CSS codes (a.k.a. subspace or stabilizer codes). The latter is a special class of CSS codes such that the stabilizer and the gauge groups are the same. In other words, a stabilizer group CSS(\mathcal{A}, \mathcal{B}) defines a regular CSS code iff $\mathcal{A} = \dot{\mathcal{B}}$ and $\mathcal{B} = \dot{\mathcal{A}}$. Note that applying the dot operation twice gives the original subspace, $\ddot{\mathcal{A}} = \mathcal{A}$, whenever $\mathcal{A} \subseteq \mathcal{E}$ and n is odd. Thus $\mathcal{A} = \dot{\mathcal{B}}$ iff $\mathcal{B} = \dot{\mathcal{A}}$. A regular CSS code has a two-dimensional codespace with an orthonormal basis

$$|0_L\rangle = |\mathcal{A}|^{-1/2} \sum_{f \in \mathcal{A}} |f\rangle \quad \text{and} \quad |1_L\rangle = X_L |0_L\rangle = |\mathcal{A}|^{-1/2} \sum_{f \in \mathcal{A}} |f + \bar{1}\rangle, \quad (10)$$

such that $\Pi = |0_L\rangle\langle 0_L| + |1_L\rangle\langle 1_L|$. In the case of subsystem CSS codes, the gauge group is strictly larger than the stabilizer group, so that the codespace can be further decomposed into a tensor product of a logical subsystem and a gauge subsystem.

4 Transversal logical gates

In this section we state sufficient conditions under which a quantum code of CSS type has transversal logical gates. Recall that a single-qubit unitary gate V is called transversal if there exist a product unitary operator $U_{all} = U_1 \otimes U_2 \otimes \dots \otimes U_n$ that preserves the codespace and the action of U_{all} on the logical qubit coincides with V . More precisely, let $\rho_L(\eta)$ be a logical state that encodes a single-qubit state η , see Eq. (5). Then we require that $U_{all} \rho_L(\eta) U_{all}^{-1} = \rho_L(V \eta V^{-1})$ for all η . To simplify

notations, we shall write $U_{all} = \prod_{j=1}^n U_j$ meaning that U_j acts on the j -th qubit. We shall use the following set of single-qubit logical gates:

$$H = \frac{1}{\sqrt{2}} \begin{bmatrix} 1 & 1 \\ 1 & -1 \end{bmatrix}, \quad S = \begin{bmatrix} 1 & 0 \\ 0 & i \end{bmatrix}, \quad \text{and} \quad T = \begin{bmatrix} 1 & 0 \\ 0 & e^{i\pi/4} \end{bmatrix}.$$

It is known that H and S generate the full Clifford group on one qubit, whereas H, S, T is a universal set generating a dense subgroup of the unitary group. The set H, S, T is known as the Clifford+ T basis. To state sufficient conditions for transversality we shall need notions of a doubly-even and a triply-even subspace [20].

Definition 1. A subspace $\mathcal{A} \subseteq \mathbb{F}_2^n$ is doubly-even iff there exist disjoint subsets $M^\pm \subseteq [n]$ such that

$$|f \cap M^+| - |f \cap M^-| = 0 \pmod{4} \quad \text{for all } f \in \mathcal{A}. \quad (11)$$

Definition 2. A subspace $\mathcal{A} \subseteq \mathbb{F}_2^n$ is triply-even iff there exist disjoint subsets $M^\pm \subseteq [n]$ such that

$$|f \cap M^+| - |f \cap M^-| = 0 \pmod{8} \quad \text{for all } f \in \mathcal{A}. \quad (12)$$

We require that at least one of the subsets M^\pm is non-empty, since otherwise the definitions are meaningless. Below we implicitly assume that each doubly- or triply-even subspace is equipped with a pair of subsets M^\pm satisfying Eq. (11) or Eq. (12) respectively. In this case \mathcal{A} is said to be doubly- or triply-even with respect to M^\pm . The original definition of triply-even codes given in [20] is recovered by choosing $M^+ = [n]$ and $M^- = \emptyset$.

Consider a pair of disjoint subsets $M^\pm \subseteq [n]$ such that

$$m = |M^+| - |M^-| = 1 \pmod{2}$$

and define n -qubit product operators

$$T_{all} = \prod_{j \in M^+} T_j \cdot \prod_{j \in M^-} T_j^{-1}, \quad S_{all} = \prod_{j \in M^+} S_j \cdot \prod_{j \in M^-} S_j^{-1}, \quad \text{and} \quad H_{all} = \prod_{j=1}^n H_j. \quad (13)$$

The following lemma provides sufficient conditions for transversality of T, S , and H gates.

Lemma 1. Consider a quantum code $\text{CSS}(\mathcal{A}, \mathcal{B})$, where $\mathcal{A}, \mathcal{B} \subseteq \mathbb{F}_2^n$ are mutually orthogonal subspaces satisfying Eq. (3). The code has a transversal gate T^m ,

$$T_{all} \rho_L(\eta) T_{all}^{-1} = \rho_L(T^m \eta T^{-m}), \quad (14)$$

whenever $\mathcal{B} = \dot{\mathcal{A}}$ and \mathcal{A} is triply even with respect to M^\pm . The code has a transversal gate S^m ,

$$S_{all} \rho_L(\eta) S_{all}^{-1} = \rho_L(S^m \eta S^{-m}), \quad (15)$$

whenever $\mathcal{A} \subseteq \mathcal{B}$ and \mathcal{A} is doubly even with respect to M^\pm . The code has a transversal H -gate,

$$H_{all} \rho_L(\eta) H_{all} = \rho_L(H \eta H), \quad (16)$$

whenever $\mathcal{A} = \mathcal{B}$.

Proof. We start from Eq. (14). Since $\mathcal{B} = \dot{\mathcal{A}}$, the codespace is two-dimensional with an orthonormal basis $|0_L\rangle, |1_L\rangle$ defined in Eq. (10). Clearly, $T_{all}|f\rangle = e^{i\pi/4(|f\cap M^+|-|f\cap M^-|)}|f\rangle$ for any basis state $|f\rangle$ of n -qubits. Combining this identity and definition of the logical state $|0_L\rangle$ one gets

$$T_{all}|0_L\rangle = T_{all} \sum_{f \in \mathcal{A}} |f\rangle = \sum_{f \in \mathcal{A}} e^{i\pi/4(|f\cap M^+|-|f\cap M^-|)} |f\rangle = |0_L\rangle.$$

Here we ignored the normalization of $|0_L\rangle$. Using the identity $|(f + \bar{1}) \cap M^\pm| = |M^\pm| - |f \cap M^\pm|$ and definition of the logical state $|1_L\rangle$ one gets

$$T_{all}|1_L\rangle = T_{all} \sum_{f \in \mathcal{A}} |f + \bar{1}\rangle = e^{i\pi m/4} \sum_{f \in \mathcal{A}} e^{-i\pi/4(|f\cap M^+|-|f\cap M^-|)} |f + \bar{1}\rangle = e^{i\pi m/4}|1_L\rangle.$$

This proves Eq. (14). Consider now Eq. (15). Let $\mathcal{H} \equiv \text{CSS}(\mathcal{A}, \mathcal{B})$ be the stabilizer group. First we claim that \mathcal{H} is invariant under the conjugated action of S_{all} , that is,

$$S_{all} \mathcal{H} S_{all}^{-1} = \mathcal{H}. \quad (17)$$

Indeed, since S_{all} commutes with Z -type stabilizers, it suffices to check that $S_{all}X(f)S_{all}^{-1} \in \mathcal{H}$ for all $f \in \mathcal{A}$. Using the identities $SXS^{-1} = iXZ$ and $S^{-1}XS = -iXZ$ one gets

$$S_{all}X(f)S_{all}^{-1} = i^{|f\cap M^+|-|f\cap M^-|} X(f)Z(f) = X(f)Z(f) \in \mathcal{H}.$$

Here we used the assumption that \mathcal{A} is doubly even and $\mathcal{A} \subseteq \mathcal{B}$ which implies $Z(f) \in \mathcal{H}$ for any $f \in \mathcal{A}$. This proves Eq. (17). We conclude that S_{all} preserves the codespace, $S_{all}\Pi S_{all}^{-1} = \Pi$. Therefore

$$S_{all} X_L \Pi S_{all}^{-1} = S_{all} X_L S_{all}^{-1} \Pi = i^m X_L Z_L \Pi \quad \text{and} \quad S_{all} Z_L \Pi S_{all}^{-1} = Z_L \Pi.$$

The assumption that m is odd implies $S^m X S^{-m} = i^m X Z$ and $S^m Z S^{-m} = Z$. We conclude that S_{all} implements a gate S^m on the logical qubit which proves Eq. (15).

The same arguments as above show that $H_{all}\Pi H_{all} = \Pi$. Since H_{all} interchanges the logical operators X_L and Z_L , this proves Eq. (16). \square

We note that $T = T^p S^q Z^r$ whenever the integers p, q, r obey $p + 2q + 4r = 1 \pmod{8}$. Using this identity one can implement the logical T -gate as a composition of the gate T^p with any odd p , the gate S^q with any odd q , and the logical Pauli operator Z_L .

5 Commuting Pauli errors through T -gates

Consider a regular code $\text{CSS}(\mathcal{A}, \mathcal{B})$ with the logical states $|0_L\rangle, |1_L\rangle$ and suppose the code has a transversal T -gate that can be implemented by a product operator $T_{all} = T^{\otimes n}$. Let $|\psi\rangle = \alpha|0_L\rangle + \beta|1_L\rangle$ be some logical state and $\rho = |\psi\rangle\langle\psi|$. In the absence of errors T_{all} preserves the codespace, so that $\eta \equiv T_{all}\rho T_{all}^\dagger$ is also a logical state. Consider now a memory error $X(e)$. Our goal is understand what

happens when T_{all} is applied to a corrupted state $X(e)\rho X(e)$. We will show that a composition of T_{all} and a certain Pauli twirling map transforms the initial state $X(e)\rho X(e)$ to a probabilistic mixture of states $E\eta E^\dagger$, where $E = X(e)Z(f)$ and $f \subseteq e$ is random vector drawn from a suitable probability distribution $P(f|e)$. However, this is true only if the initial error e satisfies a technical condition that we call *cleanability*. To state this condition, represent the binary space \mathbb{F}_2^n as a disjoint union of cosets of \mathcal{A} . By definition, each coset is a set of vectors $e + \mathcal{A}$ for some $e \in \mathbb{F}_2^n$. Since ρ is stabilized by $X(\mathcal{A})$, the state $X(e)\rho X(e)$ depends only on the coset $e + \mathcal{A}$.

Definition 3. *A coset of \mathcal{A} is cleanable iff it has a representative e such that no vector $g \in \mathcal{A}^\perp \cap \mathcal{O}$ has support inside e .*

Recall that the set $\mathcal{A}^\perp \cap \mathcal{O}$ describes undetectable non-trivial Z -errors. Thus a coset is cleanable iff it has a representative whose support contains no such errors. In particular, a coset is cleanable whenever it has a representative of weight less than $d(\mathcal{A})$, see Eq. (1). In practice, one can create a list of all cleanable cosets by examining all vectors $e \in \mathbb{F}_2^n$ and checking whether a set $M(e) \equiv \{g \in \mathcal{O}^{|e|} : g[e] \in \mathcal{A}^\perp\}$ is non-empty. The set $M(e)$ is determined by a linear system over \mathbb{F}_2 with $|e|$ variables and $1 + \dim(\mathcal{A})$ equations. If $M(e)$ is empty, the coset $e + \mathcal{A}$ is marked as cleanable. Cosets remaining unmarked at the end of this process are not cleanable.

From now on we assume that the coset $e + \mathcal{A}$ is cleanable and e is a representative that obeys the condition of Definition 3. Define a twirling map $W_{\mathcal{A}}$ that applies a random X -stabilizer drawn from the uniform distribution,

$$W_{\mathcal{A}}(\omega) = \frac{1}{|\mathcal{A}|} \sum_{g \in \mathcal{A}} X(g)\omega X(g).$$

Note that $W_{\mathcal{A}}$ has trivial action on any logical state. Consider states

$$\eta = T_{all}\rho T_{all}^\dagger \quad \text{and} \quad \tilde{\eta} = W_{\mathcal{A}}(T_{all}X(e)\rho X(e)T_{all}^\dagger).$$

The identity $TXT^\dagger = e^{i\pi/4}XS^\dagger$ implies $T_{all}X(e)T_{all}^\dagger \sim X(e)S^\dagger(e)$, where \sim stands for some phase factor. Thus

$$\tilde{\eta} = W_{\mathcal{A}}(X(e)S(e)^\dagger \eta S(e)X(e)). \quad (18)$$

Next, the identity $S \sim (I - iZ)/\sqrt{2}$ implies

$$S^\dagger(e) \sim 2^{-|e|/2} \sum_{f \subseteq e} i^{|f|} Z(f),$$

where $f \subseteq e$ is a shorthand for $\text{supp}(f) \subseteq \text{supp}(e)$. This yields

$$X(e)\tilde{\eta}X(e) = 2^{-|e|} \sum_{f, f' \subseteq e} i^{|f|-|f'|} W_{\mathcal{A}}(Z(f)\eta Z(f')).$$

We note that η is invariant under all stabilizers $X(g)$ that appear in the twirling map since it is a logical state. Commuting a stabilizer $X(g)$ from the twirling map towards η gives an extra phase

factor $(-1)^{g(f+f')}$. Summing up this phase factor over $g \in \mathcal{A}$ gives a non-zero contribution only if $f + f' \in \mathcal{A}^\perp$. This shows that

$$X(e)\tilde{\eta}X(e) = 2^{-|e|} \sum_{\substack{f, f' \subseteq e \\ f+f' \in \mathcal{A}^\perp}} i^{|f|-|f'|} Z(f)\eta Z(f'). \quad (19)$$

By cleanability assumption, the sum in Eq. (19) gets non-zero contributions only from the terms with $f + f' \in \mathcal{A}^\perp \cap \mathcal{E} \equiv \dot{\mathcal{A}}$. Furthermore, $\dot{\mathcal{A}} = \mathcal{B}$ since we assumed that the code is regular. Define a subspace

$$\mathcal{B}(e) = \{g \in \mathcal{B} : g \subseteq e\}.$$

Performing a change of variables $f' = f + g$ in Eq. (19) gives

$$X(e)\tilde{\eta}X(e) = 2^{-|e|} \sum_{f \subseteq e} \sum_{g \in \mathcal{B}(e)} i^{|f|-|f+g|} Z(f)\eta Z(f).$$

Here we noted that $\eta Z(f + g) = \eta Z(f)$ since $Z(g)$ is a stabilizer and η is a logical state. Next, the identity $|f + g| = |f| + |g| - 2|f \cap g|$ implies $i^{|f|-|f+g|} = (-1)^{f^\top g + |g|/2}$. Note that $|g|$ is even since $\mathcal{B} \subseteq \mathcal{E}$. We conclude that

$$X(e)\tilde{\eta}X(e) = 2^{-|e|} \sum_{f \subseteq e} |\mathcal{B}(e)|^{-1} \sum_{g, h \in \mathcal{B}(e)} (-1)^{f^\top g + h^\top g + |g|/2} Z(f)\eta Z(f).$$

Here we introduced a dummy variable $h \in \mathcal{B}(e)$ and used the fact that η is invariant under stabilizers $Z(h)$ with $h \in \mathcal{B}(e)$. The sum over h gives a non-zero contribution only if $g \in \mathcal{B}(e)^\perp$. We arrive at

$$X(e)\tilde{\eta}X(e) = \sum_{f \subseteq e} P(f|e) Z(f)\eta Z(f), \quad (20)$$

where

$$P(f|e) = 2^{-|e|} \sum_{g \in \mathcal{B}(e) \cap \mathcal{B}(e)^\perp} (-1)^{f^\top g + |g|/2}. \quad (21)$$

We claim that $P(f|e)$ is a normalized probability distribution on the set of vectors $f \subseteq e$, that is,

$$\sum_{f \subseteq e} P(f|e) = 1 \quad \text{and} \quad P(f|e) \geq 0.$$

Indeed, normalization of $P(f|e)$ follows trivially from Eq. (21). To prove that $P(f|e) \geq 0$ choose an arbitrary basis $\mathcal{B}(e) \cap \mathcal{B}(e)^\perp = \langle g^1, \dots, g^m \rangle$. For any vector $g = \sum_{a=1}^m x_a g^a$ one has

$$|g| = \sum_{a=1}^m x_a |g^a| - 2 \sum_{1 \leq a < b \leq m} x_a x_b |g^a \cap g^b| = \sum_{a=1}^m x_a |g^a| \pmod{4}$$

since all overlaps $|g^a \cap g^b|$ must be even. It follows that

$$P(f|e) = 2^{-|e|} \prod_{a=1}^m [1 + (-1)^{f^T g^a + |g^a|/2}] \geq 0. \quad (22)$$

To conclude, the transversal operator T_{all} followed by the twirling map transforms the initial error $X(e)$ to a probabilistic mixture of errors $X(e)Z(f)$, where $f \subseteq e$ is drawn from the distribution $P(f|e)$. However, this is true only if the coset $e + \mathcal{A}$ is cleanable. More generally, the initial state may have an error $X(e)Z(g)$. Since Z -type errors commute with T_{all} , the final error becomes $X(e)Z(g+f)$, where $f \subseteq e$ is a random vector as above.

The above discussion implicitly assumes that the initial error $X(e)$ already includes a recovery operator applied by the decoder to correct the preceding memory errors. Ideally, the recovery cancels the error modulo stabilizers. In this case $X(e)$ itself is a stabilizer and the transversal gate T_{all} creates no additional errors. If $X(e)$ is not a stabilizer but the coset $e + \mathcal{A}$ is cleanable, application of T_{all} can possibly create new errors $Z(f)$ with $f \subseteq e$. However, all these new Z -errors are either detectable or trivial due to the cleanability assumption. Thus, if the decoder has a sufficiently small list of candidate initial errors $X(e)$, it might be possible to correct the new Z -errors at the later stage. On the other hand, if the coset $e + \mathcal{A}$ is not cleanable, at least one of the new Z -errors is undetectable and non-trivial, so the the encoded information is lost. Although the decoder cannot test cleanability condition, this can be easily done in numerical simulations where the actual error is known at each step. A good strategy is to test the cleanability condition prior to each application of the logical T -gate and abort the simulation whenever the test fails. Conditioned on passing the cleanability test at each step, the only effect of the transversal gates T_{all} is to propagate pre-existing X -errors to new Z -errors as described above. In this way the simulation can be performed using the standard stabilizer formalism, even though the circuit may contain non-Clifford gates.

6 Maximum likelihood error correction and gauge fixing

In this section we develop error correction and gauge fixing algorithms for simulation of logical Clifford+ T circuits in a presence of noise. A fault-tolerant protocol implementing such logical circuit is modeled as a sequence of the following elementary steps:

- Memory errors,
- Noisy syndrome measurements,
- Code deformations extending the gauge group to a larger group,
- Code deformations restricting the gauge group to a subgroup,
- Transversal logical Clifford gates,
- Transversal logical T -gates.

We shall label steps of the protocol by an integer time variable $t = 0, 1, \dots, L$. At each step t the logical state is encoded by a quantum code of CSS type with a stabilizer group \mathcal{S}_t and a gauge group \mathcal{G}_t defined as

$$\mathcal{S}_t = \text{CSS}(\mathcal{A}_t, \mathcal{B}_t) \quad \text{and} \quad \mathcal{G}_t = \text{CSS}(\dot{\mathcal{B}}_t, \dot{\mathcal{A}}_t).$$

Each code has one logical qubit with logical Pauli operators $X_L = X(\bar{1})$, $Z_L = Z(\bar{1})$ and n physical qubits. A state of the physical qubits at the t -th step will be represented as $E_t \omega_t E_t^\dagger$, where ω_t is some logical state of the code \mathcal{S}_t and E_t is a Pauli error. To simplify notations, we shall represent n -qubit Pauli operators $X(a)Z(b)$ by binary vectors $e \in \mathbb{F}_2^{2n}$ such that $e = (a, b)$. Here we ignore the overall phase. Multiplication in the Pauli group corresponds to addition in \mathbb{F}_2^{2n} . Each Pauli error $e \in \mathbb{F}_2^{2n}$ is contained in some coset of the gauge group \mathcal{G}_t , namely, $e + \mathcal{G}_t$. The decoder described below operates on the level of cosets without ever trying to distinguish errors from the same coset. This is justified since the logical state ω_t is invariant under gauge operators, see Section 3. We shall parameterize cosets of \mathcal{G}_t by binary vectors as follows. Let A_t and B_t be some fixed generating matrices of subspaces $\mathcal{A}_t + \langle \bar{1} \rangle$ and $\mathcal{B}_t + \langle \bar{1} \rangle$. Define a matrix

$$C_t = \begin{bmatrix} B_t & \\ & A_t \end{bmatrix}. \quad (23)$$

Then the coset of a Pauli error $e = (a, b)$ is parameterized by a vector $f = C_t e = (B_t a, A_t b)$. Note that the matrix C_t has size $c_t \times 2n$, where $c_t = 2 + \dim(\mathcal{S}_t)$. Accordingly, the gauge group \mathcal{G}_t has 2^{c_t} cosets. Furthermore, if $\text{CSS}(\mathcal{A}_t, \mathcal{B}_t)$ is a regular code, that is, $\mathcal{A}_t = \dot{\mathcal{B}}_t$ and $\mathcal{B}_t = \dot{\mathcal{A}}_t$ then A_t and B_t become generating matrices of \mathcal{B}_t^\perp and \mathcal{A}_t^\perp respectively. In this case $B_t a$ determines the coset of \mathcal{A}_t that contains a while $A_t b$ determines the coset of \mathcal{B}_t that contains b . Furthermore, $c_t \leq n + 1$ with the equality in the case of regular codes.

We assume that memory errors occur at half-integer times $t - 1/2$, where $t = 1, \dots, L$. A memory error is modeled by a random vector $e \in \mathbb{F}_2^{2n}$ drawn from some fixed probability distribution π . For example, the depolarizing noise that independently applies one of the Pauli operators X, Y, Z to each qubit with probability $p/3$ can be described by $\pi(e) = \prod_{j=1}^n \pi_1(e_j, e_{n+j})$, where $\pi_1(0, 0) = 1 - p$ and $\pi_1(1, 0) = \pi_1(0, 1) = \pi_1(1, 1) = p/3$. Let $e^t \in \mathbb{F}_2^{2n}$ be the memory error that occurred at time $t - 1/2$ and $e^1 + \dots + e^t$ be the accumulated error at the t -th step. Assuming that $e \in \mathbb{F}_2^{2n}$ is drawn from the distribution π , the corresponding coset $f = C_t e$ is drawn from a distribution

$$P_t(f) = \sum_{e: C_t e = f} \pi(e). \quad (24)$$

The coset of \mathcal{G}_t that contains the accumulated error at the t -th step is

$$f^t = C_t(e^1 + e^2 + \dots + e^t). \quad (25)$$

Syndrome measurements occur at integer times $t = 1, 2, \dots, L$. The measurement performed at the t -th step determines syndromes for some subset of b_t stabilizers from the stabilizer group \mathcal{S}_t . These stabilizers may or may not be independent. They may or may not generate the full group \mathcal{S}_t .

The syndrome measurement reveals a partial information about the coset of the accumulated error f^t which can be represented by a vector

$$s^t = M_t f^t \in \mathbb{F}_2^{b_t}$$

for some binary matrix M_t of size $b_t \times c_t$. We shall refer to the vector s^t as a *syndrome*. A precise form of the matrix M_t is not important at this point. The only restriction that we impose is that $M_t C_t e = 0$ if e represents a logical Pauli operator, that is, $e = (\bar{1}, \bar{0})$ or $e = (\bar{0}, \bar{1})$. This ensures that syndrome measurements do not affect the logical qubit. In a presence of measurement errors the observed syndrome may differ from the actual one. We model a measurement error by a random vector $e' \in \mathbb{F}_2^{b_t}$ drawn from some fixed probability distribution Q_t such that the syndrome observed at the t -th step is $s^t = M_t f^t + e'$. The family of matrices C_t, M_t and the probability distributions P_t, Q_t capture all features of the error model that matter for the decoder. The decoding problem can be stated as follows.

ML Decoding: *Given a list of observed syndromes s^1, \dots, s^L , determine which coset of the gauge group \mathcal{G}_L is most likely to contain the accumulated error at the last time step.*

Below we describe an implementation of the ML decoder with the running time $O(Lc2^c)$, where $c = \max_t c_t$. The decoder can be used in the online regime such that the syndrome s^t is revealed only at the time step t . In this setting the running time is $O(c2^c)$ per time step. The decoder also includes a preprocessing step that computes matrices C_t, M_t , the effective error model P_t, Q_t , and certain additional data required for implementation of logical T -gates. The preprocessing step takes time $2^{O(n)}$ in the worst case. Since this step does not depend on the measured syndromes, it can be performed offline. The preprocessing can be done more efficiently if the code has a special structure.

Consider first the simplest case when all codes are the same and no logical gates are applied. Our model then describes a quantum memory with one logical qubit. Since all codes are the same, we temporarily suppress the subscript t in $\mathcal{G}_t, C_t, M_t, P_t, Q_t$ and c_t, b_t . For simplicity, we assume that the initial state at time $t = 0$ has no errors, that is, $f^0 = \bar{0}$. Consider some time step t and let $f \in \mathbb{F}_2^c$ be a coset of \mathcal{G} . Let $\rho_t(f)$ be the probability that f contains the accumulated error at the t -th step, $f = C(e^1 + \dots + e^t)$, conditioned on the observed syndromes s^1, \dots, s^t . Since we assume that all errors occur independently, one has

$$\rho_t(f) = \sum_{f^1, \dots, f^{t-1} \in \mathbb{F}_2^c} \prod_{u=1}^t P(f^u + f^{u-1}) \prod_{u=1}^t Q(s^u + M f^u), \quad (26)$$

where we set $f^t \equiv f$ and $f^0 \equiv \bar{0}$. Also we ignore the overall normalization of $\rho_t(f)$ which depends only on the observed syndromes. We set $\rho_0(f) = 1$ if $f = \bar{0}$ and $\rho_0(f) = 0$ otherwise. It will be convenient to represent the probability distribution $\rho_t(f)$ by a *likelihood vector*

$$|\rho_t\rangle = \sum_{f \in \mathbb{F}_2^c} \rho_t(f) |f\rangle \quad (27)$$

that belongs to the Hilbert space of c qubits. Define c -qubit operators

$$P = \sum_{f,g \in \mathbb{F}_2^c} P(f+g)|f\rangle\langle g| \quad \text{and} \quad Q_t = \sum_{f \in \mathbb{F}_2^c} Q(s^t + Mf)|f\rangle\langle f|. \quad (28)$$

Then

$$|\rho_t\rangle = (Q_t P) \cdots (Q_2 P)(Q_1 P)|\bar{0}\rangle.$$

Next we observe that P commutes with any X -type Pauli operator,

$$\langle f|X(h)P|g\rangle = \langle f+h|P|g\rangle = P(f+g+h) = \langle f|P|g+h\rangle = \langle f|PX(h)|g\rangle.$$

Thus P is diagonal in the X -basis $\{H|f\rangle\}$, where H is the Walsh-Hadamard transform on c qubits,

$$H|f\rangle = 2^{-c/2} \sum_{g \in \mathbb{F}_2^c} (-1)^{f^\top g} |g\rangle.$$

Note that $H^2 = I$. The above shows that a matrix $\hat{P} \equiv HPH$ is diagonal in the Z -basis,

$$\hat{P}|f\rangle = \hat{P}(f)|f\rangle, \quad \text{where} \quad \hat{P}(f) = \sum_{g \in \mathbb{F}_2^c} (-1)^{f^\top g} P(g). \quad (29)$$

Assuming that the likelihood vector ρ_{t-1} has been already computed and stored in a classical memory as a real vector of size 2^c , one can compute ρ_t in four steps:

1. Apply the Walsh-Hadamard transform H .
2. Apply the diagonal matrix \hat{P} .
3. Apply the Walsh-Hadamard transform H .
4. Apply the diagonal matrix Q_t .

Obviously, steps (2,4) take time $O(2^c)$. Using the fast Walsh-Hadamard transform one can implement steps (1,3) in time $O(c2^c)$. Overall, computing all likelihood vectors ρ_1, \dots, ρ_L requires time $O(Lc2^c)$. Finally, the most likely coset of \mathcal{G} at the final time step is $m^L \equiv \arg \max_f \rho_L(f)$. It can be found in time $O(2^c)$. If one additionally assumes that the final syndrome measurement is noiseless, there are only four cosets consistent with the final syndrome s^L . In this case the most likely coset m^L can be computed in time $O(1)$.

Less formally, the ML decoding can be viewed as a competition between two opposing forces. Memory errors described by P -matrices tend to spread the support of the likelihood vector over many cosets, whereas syndrome measurements described by Q -matrices tend to localize the likelihood vector on cosets f whose syndrome Mf is sufficiently close to the observed one. Typically, the most likely coset m^L coincides with the coset of the accumulated error if the likelihood vector ρ_t remains

sufficiently peaked at all time steps. Once the likelihood vector becomes flat, a successful decoding might not be possible and the encoded information is lost.

Next let us extend the ML decoder to code deformations that can change the gauge group \mathcal{G}_t , see Section 3. For concreteness, assume that a code deformation mapping \mathcal{G}_{t-1} to \mathcal{G}_t occurs at time $t - 1/4$. We assume that for any time step t one has either $\mathcal{G}_{t-1} \subseteq \mathcal{G}_t$ or $\mathcal{G}_{t-1} \supseteq \mathcal{G}_t$. The general case can be reduced to one of these cases by adding a dummy time step with a gauge group $\mathcal{G}_{t-1} \cap \mathcal{G}_t$, such that first \mathcal{G}_{t-1} is reduced to $\mathcal{G}_{t-1} \cap \mathcal{G}_t$ and next $\mathcal{G}_{t-1} \cap \mathcal{G}_t$ is extended to \mathcal{G}_t .

Case 1: $\mathcal{G}_{t-1} \subseteq \mathcal{G}_t$. Then each coset of \mathcal{G}_{t-1} uniquely determines a coset of \mathcal{G}_t . In other words, $f^t = D_t f^{t-1}$ for some binary matrix D_t of size $c_t \times c_{t-1}$. Note that $c_t \leq c_{t-1}$ since a larger group has fewer cosets. Then the code deformation is equivalent to updating the likelihood vector according to

$$|\rho_t\rangle \leftarrow \sum_{f \in \mathbb{F}_2^{c_{t-1}}} \rho_t(f) |D_t f\rangle. \quad (30)$$

Let us show that the updated vector can be computed in time $O(2^{c_{t-1}})$. Indeed, for any fixed $g \in \mathbb{F}_2^{c_t}$ a linear system $D_t f = g$ has $2^{c_{t-1}-c_t}$ solutions $f \in \mathbb{F}_2^{c_{t-1}}$. One can create a list of all solutions f and sum up the amplitudes $\rho_t(f)$ in time $O(2^{c_{t-1}-c_t})$. This would give a single amplitude of the updated likelihood vector. Since the number of such amplitudes is 2^{c_t} , the overall time scales as $O(2^{c_{t-1}})$. A good strategy for numerical simulations is to choose matrices C_t in Eq. (23) such that C_t is obtained from C_{t-1} by removing a certain subset of $c_{t-1} - c_t$ rows. Then f^t is obtained from f^{t-1} by erasing a certain subset of bits and the update Eq. (30) amounts to taking a partial trace.

Case 2: $\mathcal{G}_{t-1} \supseteq \mathcal{G}_t$. Note that $c_t \geq c_{t-1}$ since a smaller group has more cosets. Then each coset of \mathcal{G}_{t-1} splits into $2^{c_t-c_{t-1}}$ cosets of \mathcal{G}_t . Thus $f^t = D_t f^{t-1}$ for some binary matrix D_t of size $c_{t-1} \times c_t$. As we argued in Section 3, the coset f^t is drawn from the uniform distribution on the set of all cosets of \mathcal{G}_t contained in f^{t-1} , see Eq. (9). Then the code deformation is equivalent to updating the likelihood vector according to

$$|\rho_t\rangle \leftarrow 2^{c_{t-1}-c_t} \sum_{f \in \mathbb{F}_2^{c_t}} \rho_t(D_t f) |f\rangle. \quad (31)$$

The same arguments as above show that the update can be performed in time $O(2^{c_t})$. A good strategy for numerical simulations is to choose matrices C_t in Eq. (23) such that C_t is obtained from C_{t-1} by adding a certain subset of $c_t - c_{t-1}$ rows. Then f^t is obtained from f^{t-1} by inserting random bits on a subset of coordinates and the action of \tilde{D}_t on the likelihood vector amounts to taking a tensor product with the maximally mixed state of $c_t - c_{t-1}$ qubits.

Next let us discuss transversal logical gates. For concreteness, assume that a logical gate applied at a step t occurs at time $t + 1/4$, where $t = 0, \dots, L - 1$. A logical gate can be applied at a step t only if the corresponding code is regular, that is, $\mathcal{S}_t = \mathcal{G}_t = \text{CSS}(\mathcal{A}_t, \mathcal{B}_t)$, where $\mathcal{B}_t = \dot{\mathcal{A}}_t$. We only allow logical gates from the Clifford+ T basis and assume that the code \mathcal{S}_t obeys transversality conditions of Lemma 1. Let V be one of the transversal operators $H_{all}, S_{all}, T_{all}$ defined in Section 4.

We start from logical Clifford gates. Let P_t be the Pauli operator that represents the accumulated error $e^1 + \dots + e^t$. The initial state before application of V has a form $P_t \omega_t P_t^\dagger$, where ω_t is a logical

state of the code \mathcal{S}_t . The final state after application of V is

$$VP_t\omega_tP_t^\dagger V^\dagger = Q_t\tilde{\omega}_tQ_t^\dagger$$

where $\tilde{\omega}_t = V\omega_tV^\dagger$ is a new logical state and $Q_t = VP_tV^\dagger$ is a new Pauli error. Thus the likelihood of a coset $P\mathcal{G}_t$ before application of V must be the same as the likelihood of a coset $Q\mathcal{G}_t$ after application of V , where P is an arbitrary Pauli error and $Q = VPV^\dagger$. Note that the coset $Q\mathcal{G}_t$ depends only on the coset of P since $V\mathcal{G}_tV^\dagger = \mathcal{G}_t$, see the proof of Lemma 1. Thus the action of V on cosets of \mathcal{G}_t defined above can be described by a linear map $v : \mathbb{F}_2^{c_t} \rightarrow \mathbb{F}_2^{c_t}$. For concreteness, assume that cosets $f \in \mathbb{F}_2^{c_t}$ are parameterized as in Eq. (23) such that an error $X(a)Z(b)$ belongs to a coset $f = (\alpha, \beta)$, where $\alpha = B_t a$ and $\beta = A_t b$. If V implements a logical H -gate then $v(\alpha, \beta) = (\beta, \alpha)$. If V implements a logical S -gate then $v(\alpha, \beta) = (\alpha, \alpha + \beta)$. One can compute the action of any other Clifford gate on cosets in a similar fashion. This shows that application of V is equivalent to updating the likelihood vector according to

$$|\rho_t\rangle \leftarrow \sum_{f \in \mathbb{F}_2^{c_t}} \rho_t(f) |vf\rangle. \quad (32)$$

This update can be performed in time $O(2^{c_t})$.

Next assume that $V = T_{all}$ is a transversal T -gate. As we argued in Section 5, it is desirable to correct pre-existing memory errors of X -type before applying the T -gate. The ML decoder performs error correction by examining the current likelihood vector ρ_t and choosing a recovery operator from the most likely coset of X -errors

$$\alpha^* = \arg \max_{\alpha} \sum_{\beta} \rho_t(\alpha, \beta). \quad (33)$$

Applying a recovery operator $X(\alpha^*)$ is equivalent to updating the likelihood vector according to

$$|\rho_t\rangle \leftarrow \sum_{\alpha, \beta} \rho_t(\alpha, \beta) |\alpha + \alpha^*, \beta\rangle.$$

This update can be performed in time $O(2^{c_t})$.

Recall that for regular CSS codes a Pauli error (a, b) belongs to a coset $(\alpha, \beta) = C_t(a, b)$, where $\alpha = B_t a$ is the coset of \mathcal{A}_t that contains a and $\beta = A_t b$ is the coset of \mathcal{B}_t that contains b . Let \mathcal{N}_t be a set of cleanable cosets of \mathcal{A}_t , see Definition 3. As we argued in Section 5, a lookup table of cleanable cosets can be computed in time $O(2^n)$ at the preprocessing step. The next step of the ML decoder is to project the likelihood vector on the subspace spanned by cleanable cosets,

$$|\rho_t\rangle \leftarrow \sum_{\alpha \in \mathcal{N}_t} \sum_{\beta} \rho_t(\alpha, \beta) |\alpha, \beta\rangle.$$

This update can be performed in time $O(2^{c_t})$.

Now the decoder is ready to apply the transversal gate T_{all} . Here we assume for simplicity that $T_{all} = T^{\otimes n}$. For each cleanable coset α let $e(\alpha) \in \mathbb{F}_2^n$ be some fixed representative of α that satisfies condition of Definition 3, that is, $B_t e(\alpha) = \alpha$ and the support of $e(\alpha)$ contains no vectors from $\mathcal{A}_t^\perp \cap \mathcal{O}$. A lookup table of vectors $e(\alpha)$ must be computed at the preprocessing step. As was argued in Section 5, a composition of T_{all} and a twirling map $\mathcal{W}_{\mathcal{A}_t}$ maps a pre-existing Pauli error $X(e)Z(g)$ to a probabilistic mixture of Pauli errors $X(e)Z(f+g)$, where $f \subseteq e$ is a random vector drawn from distribution $P(f|e)$ defined in Eqs. (21,22). Since the twirling map has no effect on the likelihood vector, it can be skipped. Thus T_{all} updates the likelihood vector according to

$$|\rho_t\rangle \leftarrow \sum_{\alpha, \beta} \sum_{f \subseteq e(\alpha)} P(f|e(\alpha)) \rho_t(\alpha, \beta) |\alpha, \beta + A_t f\rangle. \quad (34)$$

Define an auxiliary operator Γ_α such that

$$\Gamma_\alpha |\beta\rangle = \sum_{f \subseteq e(\alpha)} P(f|e(\alpha)) |\beta + A_t f\rangle. \quad (35)$$

This operator acts on the Hilbert space of m qubits, where $m = \dim(\mathcal{B}_t^\perp) = 1 + \dim(\mathcal{A}_t)$. Then Eq. (34) can be written as

$$|\rho_t\rangle \leftarrow \left(\sum_{\alpha} |\alpha\rangle\langle\alpha| \otimes \Gamma_\alpha \right) |\rho_t\rangle. \quad (36)$$

We note that Γ_α is diagonal in the X -basis since

$$\Gamma_\alpha = \sum_{f \subseteq e(\alpha)} P(f|e(\alpha)) X(A_t f).$$

Let H be the Walsh-Hadamard transform on m qubits. Define an operator $\hat{\Gamma}_\alpha = H \Gamma_\alpha H$ which is diagonal in the Z -basis of m qubits. The diagonal matrix elements of $\hat{\Gamma}_\alpha$ are

$$\langle \beta | \hat{\Gamma}_\alpha | \beta \rangle = \sum_{f \subseteq e(\alpha)} P(f|e(\alpha)) (-1)^{\beta^\top A_t f}. \quad (37)$$

Below we consider some fixed α and use a shorthand $e \equiv e(\alpha)$. Substituting the explicit expression for $P(f|e)$ from Eq. (21) into Eq. (37) yields

$$\langle \beta | \hat{\Gamma}_\alpha | \beta \rangle = \sum_{g \in \mathcal{B}_t(e) \cap \mathcal{B}_t(e)^\perp} 2^{-|e|} \sum_{f \subseteq e} (-1)^{f^\top g + |g|/2 + \beta^\top A_t f}. \quad (38)$$

The sum over f vanishes unless the restriction of the vector $A_t^\top \beta$ onto e coincides with g . Define a diagonal $n \times n$ matrix J_e that has non-zero entries in the support of e , that is, $\text{diag}(J_e) = e$. Then we get a constraint $g = J_e A_t^\top \beta$ and $g \in \mathcal{B}_t(e) \cap \mathcal{B}_t(e)^\perp$. This shows that

$$\langle \beta | \hat{\Gamma}_\alpha | \beta \rangle = \begin{cases} (-1)^{\frac{1}{2}|J_e A_t^\top \beta|} & \text{if } J_e A_t^\top \beta \subseteq \mathcal{B}_t(e) \cap \mathcal{B}_t(e)^\perp, \\ 0 & \text{otherwise.} \end{cases} \quad (39)$$

The action of the diagonal operator $\hat{\Gamma}_\alpha$ on any state of m qubits can be computed in time $O(2^m)$ using Eq. (39). Using the fast Walsh-Hadamard transform on m qubits one can compute the action of the original operator Γ_α defined in Eq. (35) on any state of m qubits in time $O(m2^m)$. The number of cleanable cosets α is upper bounded by the total number of cosets of \mathcal{A}_t . The latter is equal to 2^k , where $k = \dim(\mathcal{A}_t^\perp) = 1 + \dim(\mathcal{B}_t)$. The updated likelihood vector can be computed by evaluating each term α in Eq. (36) individually and summing up these terms. This calculation requires time $O(m2^{k+m}) = O(c_t 2^{c_t})$. Overall, application of the transversal T -gate requires time $O(c_t 2^{c_t})$.

7 Logical Clifford+ T circuits with the 15-qubit code

In this section we apply the ML decoder to a specific fault-tolerant protocol which similar to the one proposed by Anderson et al [14]. The protocol simulates a logical quantum circuit composed of Clifford and T gates by alternating between two error correcting codes: the 7-qubit color code (a.k.a. the Steane code) and the 15-qubit Reed-Muller code. We shall label these two codes C and T since they provide transversal Clifford gates and the T -gate respectively. Both C and T are regular CSS codes that can be obtained by the gauge fixing method from a single subsystem CSS code that we call the base code. This section may also serve as simple example illustrating the general construction of doubled color codes described in Sections 8-12.

Our starting point is the 7-qubit color code. Consider a graph $\Lambda = (V, E)$ with a set of vertices $V = [7]$ and a set of edges E shown on Fig. 1(a). For consistency with the subsequent sections, we shall refer to the graph Λ as a lattice. Vertices of Λ will be referred to as sites. We place one qubit at each site of the lattice. Let $f^1, f^2, f^3 \subseteq \mathbb{F}_2^7$ be the three faces of Λ , see Fig. 1(b), and $\mathcal{S} \subseteq \mathbb{F}_2^7$ be the three-dimensional subspace spanned by the faces, $\mathcal{S} = \langle f^1, f^2, f^3 \rangle$. The faces f^1, f^2, f^3 can also be viewed as rows of a parity check matrix

1		1		1		1
	1	1			1	1
			1	1	1	1

The 7-qubit color code has a stabilizer group $\text{CSS}(\mathcal{S}, \mathcal{S})$. This is a regular CSS code with six stabilizers $X(f^i), Z(f^i)$. The code distance is $d = d(\mathcal{S}) = 3$. Minimum weight logical operators are $X(\omega), Z(\omega)$, where

$$\omega = \bar{1} + f^2 = e^1 + e^4 + e^5.$$

Recall that e^i denotes the standard basis vector of the binary space. The subspace \mathcal{S} is doubly even, $|f| = 0 \pmod{4}$ for all $f \in \mathcal{S}$. Lemma 1 implies that the color code has transversal logical gates H and S that can be realized by operators $H_{all} = H^{\otimes 7}$ and $S_{all} = S^{\otimes 7}$.

Suppose now that each site of the lattice Λ contains two qubits labeled A and B . Let us add one additional qubit labeled C . We assume that C is placed next to the lattice Λ such that C and ω form one additional face, see Fig. 1(c). This defines a system of 15 qubits that are partitioned into three consecutive blocks, $[15] = ABC$, where $|A| = |B| = 7$ and $|C| = 1$.

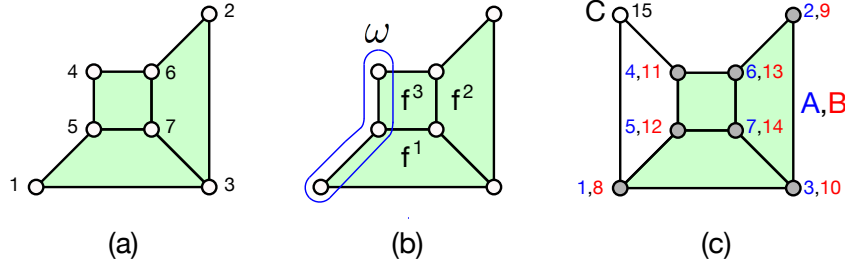


Figure 1: (a) Color code lattice Λ . The 7-qubit color code is defined by placing one qubit at each site of Λ . (b) Faces f^1, f^2, f^3 and the subset ω define stabilizers $X(f^i), Z(f^i)$ and logical operators $X(\omega), Z(\omega)$ respectively. (c) A doubled color code is obtained by making two copies of Λ labeled A and B placed atop of each other, and adding one additional qubit labeled C .

The T -code that provides a transversal T -gate has a stabilizer group $\text{CSS}(\mathcal{T}, \dot{\mathcal{T}})$, where $\mathcal{T} \subseteq \mathbb{F}_2^{15}$ is a four-dimensional subspace spanned by double faces of the lattice Λ and by the all-ones vector supported on the region BC ,

$$\mathcal{T} = \langle f^i[A] + f^i[B] \rangle + \langle BC \rangle. \quad (40)$$

Here $i = 1, 2, 3$ and $BC \equiv \bar{1}[BC]$. One can also view basis vectors of \mathcal{T} as rows of a parity check matrix

1		1		1		1		1		1		1		1
	1	1			1	1			1	1			1	1
			1	1	1	1					1	1	1	1
							1	1	1	1	1	1	1	1

Here the first three rows stand for $f^i[A] + f^i[B]$ and the last row stands for BC . A direct inspection shows that \mathcal{T} is triply even, $|f| \equiv 0 \pmod{8}$ for all $f \in \mathcal{T}$. By Lemma 1, the T -code has a transversal logical T -gate realized by an operator $T_{all} = T^{\otimes 15}$. Let us explicitly describe Z -stabilizers of the T -code. Define a subspace $\mathcal{G} \subseteq \mathbb{F}_2^{15}$ spanned by double edges of Λ ,

$$\mathcal{G} = \langle l[A] + l[B] : l \in E \rangle. \quad (41)$$

For example, a double edge $l = (2, 3) \in E$ gives rise to a basis vector $l[A] + l[B] = e^2 + e^3 + e^9 + e^{10}$, see Fig. 1(c). Clearly, double edges $l[A] + l[B]$ have an even overlap with double faces $f^i[A] + f^i[B]$ as well as with the vector BC . This shows that $\mathcal{G} \subseteq \dot{\mathcal{T}}$. Define also a subspace $\mathcal{C} \subseteq \mathbb{F}_2^{15}$ spanned by single faces of Λ , including the extra face formed by ω and C , namely

$$\mathcal{C} = \langle f^i[A] \rangle + \langle f^i[B] \rangle + \langle \omega[B] + C \rangle, \quad (42)$$

where $i = 1, 2, 3$ and $C \equiv 1[C]$. A direct inspection shows that $\mathcal{C} \subseteq \dot{\mathcal{T}}$ and, moreover,

$$\dot{\mathcal{T}} = \mathcal{C} + \mathcal{G}. \quad (43)$$

To summarize, Z -stabilizers of the T -code fall into three classes: (i) *edge-type* stabilizers $Z(f)$, where $f = l[A] + l[B]$ is a double edge of the color code lattice Λ , (ii) *face-type* stabilizers $Z(g)$, where $g = f^i[A]$ or $g = f^i[B]$ is a face of the lattice Λ , and (iii) a special face-type stabilizer $g = \omega[B] + C$ that represents the extra face connecting C and ω . These stabilizers are not independent. For example, the product of edge-type stabilizers over any closed loop on the color code lattice Λ gives the identity. Minimum weight logical operators of the T -code can be chosen as $X(A)$ and $Z(\omega[A])$. The code distance is $d = 3$ since $d(\mathcal{T}) = 3$ and $d(\dot{\mathcal{T}}) = 7$.

The C -code that provides transversal Clifford gates has a stabilizer group $\text{CSS}(\mathcal{C}, \mathcal{C})$, where \mathcal{C} is defined by Eq. (42). Stabilizers of this code can be partitioned into three classes: (i) stabilizers $X(f^i[A])$, $Z(f^i[A])$ define the 7-qubit color code on the region A with logical operators $X(\omega[A])$, $Z(\omega[A])$, (ii) stabilizers $X(f^i[B])$, $Z(f^i[B])$ define the 7-qubit color code on the region B with logical operators $X(\omega[B])$, $Z(\omega[B])$, and (c) stabilizers $X(\omega[B] + C)$, $Z(\omega[B] + C)$ define the two-qubit EPR state $|0, 0\rangle + |1, 1\rangle$ shared between B and C such that the first qubit of the EPR state is encoded by the 7-qubit color code. Thus any logical state of the C -code has a form

$$|\psi_L\rangle = (\alpha|0_L\rangle + \beta|1_L\rangle)_A \otimes (|0_L0\rangle + |1_L1\rangle)_{BC}, \quad (44)$$

where $\alpha, \beta \in \mathbb{C}$ are some coefficients and $|0_L\rangle$, $|1_L\rangle$ are the logical basis states of the 7-qubit color code. By discarding qubits of BC one can convert the C -code into the 7-qubit color code. Thus these two codes have the same logical operators, the same distance, and the same transversality properties. In particular, the C -code provides a transversal implementation of the full Clifford group. This can also be seen from Lemma 1 by noting that $\dot{\mathcal{C}} = \mathcal{C}$ and \mathcal{C} is doubly even, $|f| = 0 \pmod{4}$ for all $f \in \mathcal{C}$.

The base code appears as an intermediate step in the conversion between C and T codes. The stabilizer group of the base code is defined as the intersection of stabilizer groups $\text{CSS}(\mathcal{C}, \mathcal{C})$ and $\text{CSS}(\mathcal{T}, \dot{\mathcal{T}})$ describing the C and T codes. Thus the base code has a stabilizer group $\text{CSS}(\mathcal{C} \cap \mathcal{T}, \mathcal{C} \cap \dot{\mathcal{T}})$. By definition, $\mathcal{C} \subseteq \dot{\mathcal{T}}$, see Eq. (43), that is, $\mathcal{C} \cap \dot{\mathcal{T}} = \mathcal{C}$. We claim that $\mathcal{T} \subseteq \mathcal{C}$. Indeed, all double face generators of \mathcal{T} are contained in \mathcal{C} by definition, so we just need to check that $BC \in \mathcal{C}$. Using the identity $f^2 + \omega = \bar{1}$, see Fig. 1(a,b), one gets

$$BC = B + C = (f^2 + \omega)[B] + C = f^2[B] + (\omega[B] + C) \in \mathcal{C}. \quad (45)$$

We conclude that the base code has a stabilizer group $\text{CSS}(\mathcal{T}, \mathcal{C})$ and the gauge group $\text{CSS}(\dot{\mathcal{C}}, \dot{\mathcal{T}}) = \text{CSS}(\mathcal{C}, \dot{\mathcal{T}})$. The base code has distance $d = 3$ since $d(\mathcal{T}) = d(\mathcal{C}) = 3$. All three codes have the same logical operators defined in Eq. (4). We summarize definitions of the three codes in Table 1.

We are now ready to describe a fault-tolerant implementation of a logical circuit in the Clifford+ T basis. Our protocol consists of an alternating sequence of rounds labeled C and T , see Fig. 2. Each C -round is responsible for measuring syndromes of all face-type stabilizers of the C -code, that is, $X(f)$ and $Z(f)$, where f is one of the vectors $f^i[A]$, $f^i[B]$, or $\omega[B] + C$. Each T -round is responsible for measuring syndromes of all edge-type stabilizers of the T -code, that is, stabilizers $Z(l[A] + l[B])$ with $l \in E$. All measured syndromes are sent to the decoder. Typically, but not always, a logical Clifford gate (T -gate) is applied after each C -round (T -round). Whether or not a logical gate is applied depends on the outcome of a certain test that we call a syndrome test. A decoder is responsible for

	Transversal gates	X -stabilizers	Z -stabilizers	stabilizer group	gauge group
C -code	Clifford group	single faces	single faces	$\text{CSS}(\mathcal{C}, \mathcal{C})$	$\text{CSS}(\mathcal{C}, \mathcal{C})$
T -code	T gate	double faces BC	single faces double edges	$\text{CSS}(\mathcal{T}, \dot{\mathcal{T}})$	$\text{CSS}(\mathcal{T}, \dot{\mathcal{T}})$
Base code		double faces BC	single faces	$\text{CSS}(\mathcal{T}, \mathcal{C})$	$\text{CSS}(\mathcal{C}, \dot{\mathcal{T}})$

Table 1: The family of codes used in the protocol.

choosing a recovery operator R which is applied at the end of every pair of C, T rounds passing the syndrome test. In the beginning of each round the decoder performs a code deformation such that the logical qubit is encoded by the C -code (T -code) in every C -round (T -round). Although the base code does not explicitly appear in the protocol, it is used by the decoder as an intermediate step in the code deformation, see Section 6. Namely, at the beginning of each C -round the gauge group changes according to

$$\text{CSS}(\mathcal{T}, \dot{\mathcal{T}}) \rightarrow \text{CSS}(\mathcal{C}, \dot{\mathcal{T}}) \rightarrow \text{CSS}(\mathcal{C}, \mathcal{C}).$$

At the beginning of each T -round the gauge group changes in the reverse direction.

Let us now describe the syndrome test. Recall that the syndromes of $X(f)$ and $Z(f)$ are denoted $\xi(f)$ and $\zeta(f)$ respectively, see Section 3. Consider some fixed pair of rounds C, T and let U be the logical Clifford gate applied in the C -round (set $U = I$ if no logical gate have been applied). Let $\xi(f)$ and $\zeta(f)$ be the face-type syndromes measured in this round. Measuring the syndrome of a stabilizer $Z(f)$ after application of U is equivalent to measuring the syndrome of $P(f)$ before application of U , where $P \equiv UZU^\dagger$. Suppose $P \sim X(a)Z(b)$, where $a, b \in \mathbb{F}_2$. Define an updated syndrome

$$\zeta_U(f) = a\xi(f) + b\zeta(f).$$

Thus $\zeta_U(f)$ determines the syndrome of a stabilizer $Z(f)$ that would be observed in the absence of the logical gate U . Let $\zeta(l[A] + l[B])$ be the edge-type syndromes measured in the T -round. We say that the pair of rounds C, T passes a syndrome test if

$$\zeta(l[A] + l[B]) + \zeta(l'[A] + l'[B]) + \zeta_U(f^i[A]) + \zeta_U(f^i[B]) = 0 \quad (46)$$

for any face f^i and for any pair of edges $l, l' \in E$ such that $l + l' = f^i$. In other words, l and l' are the two opposite edges forming the boundary of f^i .

In the absence of errors the syndrome test is always passed since the product of edge-type stabilizers $Z(l[A] + l[B])$, $Z(l'[A] + l'[B])$ and face-type stabilizers $Z(f^i[A])$, $Z(f^i[B])$ equals the identity. Our protocol performs the syndrome test after each T -round, see Fig. 2. If the syndrome test fails, an additional pair of rounds C, T is requested and the process continues until the syndrome test is passed. We note that the syndrome test can fail for at least two reasons. First, any single-qubit X -error on some qubit $j \in AB$ that occurs inside the chosen T -round flips the syndromes $\zeta(l[A] + l[B])$ on all

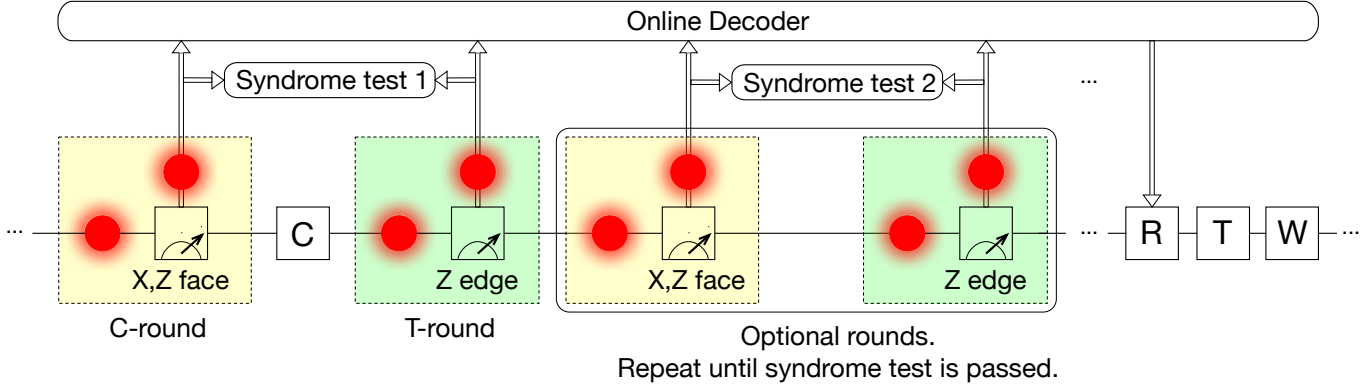


Figure 2: A fault-tolerant implementation of a Clifford+ T circuit. Red circles represent depolarizing memory errors and syndrome measurement errors. Transversal Clifford and T -gates are shown by C and T boxes. The boxes W and R represent the twirling map and the recovery operator respectively. Measurement boxes represent (partial) syndrome measurements. Face-type stabilizers of the C -code are measured in every C -round. Edge-type stabilizers of the T -code are measured in every T -round. Optional rounds are added only if the full syndrome of the T -code inferred from these measurements fails to pass a consistency test. The rounds continue in the periodic fashion. On average, the protocol applies one logical gate per round.

edges l incident to the site $u \in \Lambda$ that contains j without flipping any face-type syndromes (because the latter have been measured *before* this error occurred). This would violate at least one constraint in Eq. (46). Secondly, any single measurement error for edge-type stabilizers $Z(l[A] + l[B])$ in the T -round or any single measurement error for face-type stabilizers that contribute to the updated syndromes $\zeta_U(f)$ would violate at least one constraint in Eq. (46). The purpose of the syndrome test is to ensure that neither of these possibilities occurs before asking the decoder to perform a recovery operation.

Combining syndromes measured in any consecutive pair of rounds C, T provides the full syndrome for the T -code (in the absence of errors). Indeed, the syndrome of $X(\mathcal{T})$ can be inferred from the syndromes of $X(\mathcal{C})$ and $Z(\mathcal{C})$ measured in the C -round since $\mathcal{T} \subseteq \mathcal{C}$ and $X(\mathcal{T})$ commutes with all operators measured in the T -round. Likewise, the syndrome of $Z(\dot{\mathcal{T}})$ can be obtained by combining the syndromes of $X(\mathcal{C})$ and $Z(\mathcal{C})$ measured in the C -round and the syndrome of $Z(\mathcal{G})$ measured in the T -round, since $\dot{\mathcal{T}} = \mathcal{C} + \mathcal{G}$. By spreading the syndrome measurement for the T -code over two rounds we were able to keep the number of measurements per qubit in any single round reasonably small, which might be important for practical implementation.

A transversal Clifford gate is applied after each C -round provided that the latest syndrome tests was successful. We performed simulations for a random Clifford+ T circuit such that each Clifford gate is drawn from the uniform distribution on the Clifford group.

A transversal T -gate is applied at the end of each T -round that passes the syndrome test. It

is preceded by a Pauli recovery operator R classically controlled by the decoder, see Section 6, and followed by a twirling map $\mathcal{W}_{\mathcal{T}}$ that applies a randomly chosen stabilizer $X(f)$ with $f \in \mathcal{T}$,

$$\mathcal{W}_{\mathcal{T}}(\rho) = \frac{1}{|\mathcal{T}|} \sum_{f \in \mathcal{T}} X(f)\rho X(f). \quad (47)$$

Each round includes memory and syndrome measurement errors. We model memory errors by the depolarizing noise with some error rate p , that is, each qubit suffers from a Pauli error X, Y, Z with probability $p/3$ each. Within each round a memory error occurs before the syndrome measurement, see Fig. 2. We model a noisy syndrome measurement by an ideal measurement in which the outcome is flipped with a probability p .

At any given time step the protocol can be terminated depending on the outcome of two tests: (1) logical error test and (2) cleanability test. A logical error test is performed at the end of each round by computing the most likely coset of errors consistent with the current syndrome. The test is passed if the most likely coset contains the actual memory error. A cleanability test is performed after each recovery operation. If $E \sim X(a)Z(b)$ is the residual error left after the recovery, the test is passed if $a + \mathcal{T}$ is a cleanable coset, see Eq. (40) and Definition 3. We found that \mathcal{T} has 996 cleanable cosets. The protocol terminates whenever one of the two tests fails. Accordingly, the number of logical gates implemented in the protocol is a random variable. Conditioned on passing the cleanability test, a transversal T -gate is implemented using the method of Section 5. The quantity we are interested in is a logical error rate defined as $p_L = 1/g$, where g is the average number of logical gates implemented before the protocol terminates. Here g includes both Clifford and T gates.

The logical error rate p_L was computed numerically using a simplified version of the ML decoder that we call a sparse ML decoder (SMLD). It follows the algorithm described in Section 6 with two modifications. First, SMLD models memory errors by a sparse distribution π^s approximating the exact distribution π . We have chosen $\pi^s(e) = \pi(e)$ if e is a Pauli error acting non-trivially on at most one qubit and $\pi^s(e) = 0$ otherwise (here we ignore the normalization). Replacing π by π^s in the update rules of Section 6 one can see that the matrix P_t defined in Eqs. (24,28) becomes sparse and the update $|\rho_t\rangle \leftarrow P_t|\rho_t\rangle$ can be performed using sparse matrix-vector multiplication avoiding the Walsh-Hadamard transforms. The actual memory errors in the Monte Carlo simulation are drawn from the exact distribution π . This approximation is justified since none of the codes used in the protocol can correct memory errors of weight larger than one. Secondly, SMLD performs a truncation of the likelihood vector ρ_t after each round in order to keep ρ_t sufficiently sparse. The truncation was performed by normalizing ρ_t and setting to zero all components with $\rho_t(f) < \epsilon$, where $\epsilon = 10^{-6}$ is an empirically chosen cutoff value. We observed that for large error rates ($p \approx 1\%$) the two versions of the decoder achieve the same logical error probability within statistical fluctuations. On the other hand, SMLD provides at least 10x speedup compared with the exact version and enables simulation of circuits with more than 10,000 logical gates. Our results are presented on Fig. 3. We observed a scaling $p_L = Cp^2$ with $C \approx 182$. Assuming that a physical Clifford+ T circuit has an error probability p per gate, the logical circuit becomes more reliable than the physical one provided that $p_L < p$, that is, $p < p_0 = C^{-1} \approx 0.55\%$. This value can be viewed as an “error threshold” of the proposed protocol. Generating the data shown on Fig. 3 took approximately one day on a laptop computer.

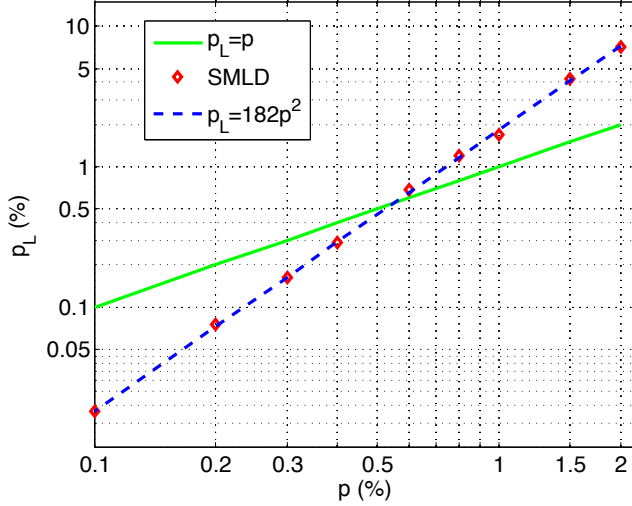


Figure 3: Monte Carlo simulation of logical Clifford+ T circuits with the sparse ML decoder (SMLD). Here p is the physical error rate and p_L is the logical error rate defined as $p_L = 1/g$, where g is the average number of logical gates implemented before the protocol terminates. Each average was estimated using 400 Monte Carlo trials.

8 Doubled color codes: main properties

Our goal for the rest of the paper is to generalize the 15-qubit codes described in Section 7 to higher distance codes that can be embedded into a 2D lattice such that all syndrome measurements required for error correction and gauge fixing are spatially local. This section highlights main properties of the new codes. Let $d = 2t + 1$ be the desired code distance, where $t \geq 1$ is an integer. For each t we shall construct a pair of CSS codes labeled C and T that encode one logical qubit into $n_t = 2t^3 + 8t^2 + 6t - 1$ physical qubits. These codes have transversal Clifford gates and the T -gate respectively. The codes are defined on the 2D honeycomb lattice with two qubits per site such that the gauge group of the C -code has spatially local generators supported on faces of the lattice. Most of these generators are analogous to face-type stabilizers in the 15-qubit example, see Section 7. There are also additional generators of weight two that couple pair of qubits located on the same face. The latter have no analogue in the 15-qubit example. The C -code can be converted to the regular color code on the honeycomb lattice by discarding a certain subset of qubits. Although the T -code does not have local gauge generators, it can be obtained from the C -code by a local gauge fixing. It requires syndrome measurements for weight-four stabilizers supported on edges of the lattice. The latter are analogous to edge-type stabilizers in the 15-qubit example. We shall also define a base code that appears as an intermediate step in the conversion between C and T codes. All three codes have distance $d = 2t + 1$.

The codes will be constructed from a pair of linear subspaces $\mathcal{C}_t, \mathcal{T}_t \subseteq \mathbb{F}_2^{n_t}$ that satisfy

$$\mathcal{T}_t \subseteq \mathcal{C}_t \subseteq \hat{\mathcal{C}}_t \subseteq \hat{\mathcal{T}}_t \quad (48)$$

and

$$d(\mathcal{T}_t) = 2t + 1. \quad (49)$$

The subspaces \mathcal{C}_t and \mathcal{T}_t have a special symmetry required for transversality of logical gates, namely, \mathcal{C}_t is doubly even and \mathcal{T}_t is triply even with respect to some subsets of qubits $M_t^\pm \subseteq [n_t]$ such that $|M_t^+| - |M_t^-| = 1$. Furthermore, $\dot{\mathcal{C}}_t$ and $\dot{\mathcal{T}}_t$ have spatially local generators (basis vectors) supported on faces of the lattice. The subspaces \mathcal{C}_1 and \mathcal{T}_1 coincide with \mathcal{C} and \mathcal{T} defined in Section 7. Definitions of the three codes are summarized in Table 2. We shall refer to the family of codes defined in Table 2 as doubled color codes since each of them is constructed from two copies of the regular color code.

	Transversal gates	Stabilizer group	Gauge group
C -code	Clifford group	$\text{CSS}(\mathcal{C}_t, \mathcal{C}_t)$	$\text{CSS}(\dot{\mathcal{C}}_t, \dot{\mathcal{C}}_t)$
T -code	T gate	$\text{CSS}(\mathcal{T}_t, \dot{\mathcal{T}}_t)$	$\text{CSS}(\mathcal{T}_t, \dot{\mathcal{T}}_t)$
Base code		$\text{CSS}(\mathcal{T}_t, \mathcal{C}_t)$	$\text{CSS}(\dot{\mathcal{C}}_t, \dot{\mathcal{T}}_t)$

Table 2: A family of 2D doubled color codes that achieves universality by the gauge fixing method. Each code has one logical qubit, $n_t = 2t^3 + 8t^2 + 6t - 1$ physical qubits, and distance $d = 2t + 1$. The subspaces $\dot{\mathcal{C}}_t$ and $\dot{\mathcal{T}}_t$ have spatially local generators supported on faces of the lattice. These subspaces are doubly even and triply even respectively.

We expect that the new codes can be used in a protocol analogous to the one shown on Fig. 2 to implement fault-tolerant Clifford+ T circuits in the 2D architecture. The C -round of the protocol would be responsible for measuring gauge syndromes $\xi(f^\alpha)$ and $\zeta(f^\alpha)$ for some complete set of generators $f^1, \dots, f^m \in \dot{\mathcal{C}}_t$. A transversal Clifford gate can be applied after each C -round. The T -round would be responsible for measuring stabilizer syndromes $\zeta(g^\beta)$ for some set of generators $g^1, \dots, g^k \in \dot{\mathcal{T}}_t$ such that $\dot{\mathcal{T}}_t = \langle f^1, \dots, f^m, g^1, \dots, g^k \rangle$. We will see that such generators g^β can be chosen as double edges of the lattice, by analogy with the 15-qubit example. A transversal T -gate can be applied after each T -round. In the case of higher distance codes the C -round could be repeated several times to ensure that any combination of t syndrome measurement errors is correctable. We expect that the T -round requires less (if any) repetitions since the edge-type stabilizers measured in this round are highly redundant. An explicit construction of a fault-tolerant protocol that would suppress the error probability per gate from p to $O(p^{t+1})$ is an interesting open problem that we leave for a future work.

9 Regular color codes

The starting point for our construction is the standard color code on the hexagonal lattice [23]. For a suitable choice of boundary conditions such code has exactly one logical qubit and corrects t single-qubit errors, where $t \geq 0$ is any given integer (recall that the code distance is $d = 2t + 1$). Examples of the color code lattice for $t \leq 3$ are shown on Fig. 4. More formally, consider a lattice Δ_t such that

the lattice sites are triples of non-negative integers $\mathbf{j} = (j_1, j_2, j_3)$ satisfying $j_1 + j_2 + j_3 = 3t$. Clearly, Δ_t is the regular triangular lattice. Note that $j_2 - j_1 = j_3 - j_2 = j_1 - j_3 \pmod{3}$ for any $\mathbf{j} \in \Delta_t$. For each $b \in \mathbb{Z}_3$ consider a sublattice

$$\Delta_t^b = \{ \mathbf{j} \in \Delta_t : j_2 - j_1 = b \pmod{3} \}. \quad (50)$$

Define a color code lattice Λ_t as

$$\Lambda_t = \Delta_t^0 \cup \Delta_t^2. \quad (51)$$

In other words, sites of Λ_t are triples of non-negative integers $\mathbf{j} = (j_1, j_2, j_3)$ satisfying $j_1 + j_2 + j_3 = 3t$ and $j_2 - j_1 \not\equiv 1 \pmod{3}$. Sites of the triangular lattice Δ_t that are not present in Λ_t become centers of faces of Λ_t . More formally, a subset $f \subseteq \Lambda_t$ is called a face iff there exists $\mathbf{j} \in \Delta_t^1$ such that f is the set of nearest neighbors of \mathbf{j} in the triangular lattice Δ_t . A direct inspection shows that any face of Λ_t consists of four or six sites. Although the color code lattice is usually equipped with a face 3-coloring, we shall not specify the colors since they are irrelevant for what follows.

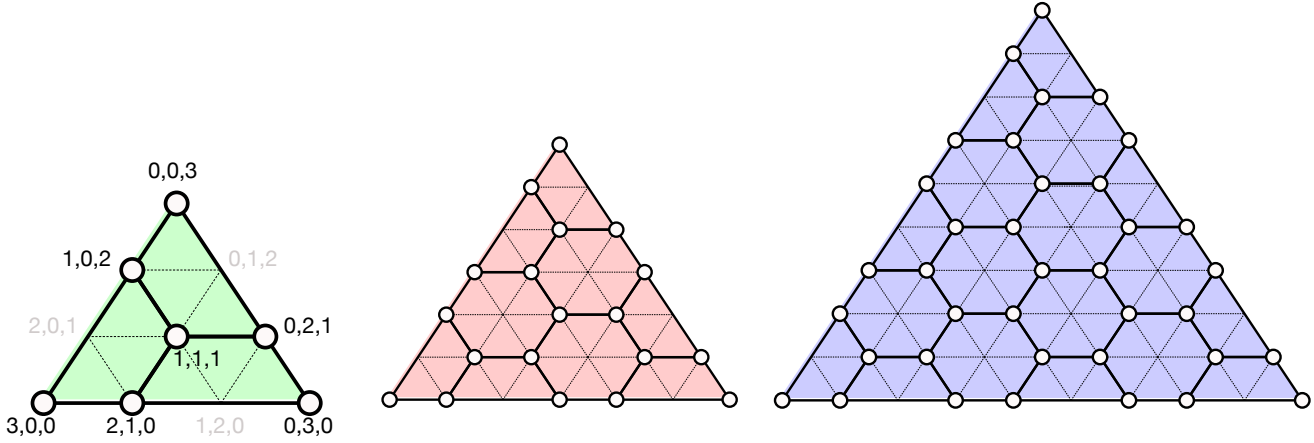


Figure 4: Color code lattices Λ_1 , Λ_2 , and Λ_3 . Qubits are located at the lattice sites (empty circles). Each face f gives rise to a pair of stabilizer generators $\hat{X}(f)$ and $\hat{Z}(f)$. The color code defined on the lattice Λ_t has one logical qubit and corrects t single-qubit errors (code distance is $d = 2t + 1$).

The lattice Λ_t contains

$$m_t = |\Lambda_t| = 3t^2 + 3t + 1 \quad (52)$$

sites and $(m_t - 1)/2$ faces. We will use a convention that Λ_0 is a single site. Let $\mathcal{S}_t \subseteq \mathbb{F}_2^{m_t}$ be a subspace spanned by all faces of Λ_t (recall that we identify a face f and a binary vector whose support is f). Note that \mathcal{S}_t is self-orthogonal, since any pair of faces overlap on even number of sites. We shall need the following well-known properties of \mathcal{S}_t , see Refs. [23, 18, 24].

Fact 1. *The subspace \mathcal{S}_t is doubly-even with respect to the subsets Δ_t^0 and Δ_t^2 . Furthermore,*

$$|\Delta_t^0| - |\Delta_t^2| = 1. \quad (53)$$

The orthogonal subspace \mathcal{S}_t^\perp is given by

$$\mathcal{S}_t^\perp \cap \mathcal{E} = \mathcal{S}_t \quad \text{and} \quad \mathcal{S}_t^\perp \cap \mathcal{O} = \mathcal{S}_t + \bar{1}, \quad (54)$$

Finally,

$$d(\mathcal{S}_t) = 2t + 1. \quad (55)$$

For the sake of completeness, let us prove the first claim.

Proof. We shall use shorthand notations $\mathcal{S} \equiv \mathcal{S}_t$, $m \equiv m_t$, and $\Delta^b \equiv \Delta_t^b$. Consider any stabilizer $f \in \mathcal{S}$. Then f is a linear combination of faces. One can always choose the numbering of faces such that $f = \sum_{i=1}^k f^i$ for some $k \leq s$. We shall use an identity

$$\left| \sum_{i=1}^k g^i \right| = \sum_{i=1}^k |g^i| - 2 \sum_{1 \leq i < j \leq k} |g^i \cap g^j| \pmod{4} \quad (56)$$

which holds for any vectors $g^1, \dots, g^k \in \mathbb{F}_2^m$. Choosing $g^i = f^i \cap \Delta^b$ one gets

$$|f \cap \Delta^0| - |f \cap \Delta^2| = \sum_{i=1}^k (|f^i \cap \Delta^0| - |f^i \cap \Delta^2|) - 2 \sum_{1 \leq i < j \leq k} (|f^i \cap f^j \cap \Delta^0| - |f^i \cap f^j \cap \Delta^2|) \quad (57)$$

modulo four. Consider any site $\mathbf{j} \in \Delta^1$. The nearest neighbors of \mathbf{j} in the triangular lattice belong to either Δ^0 or Δ^2 as shown on Fig. 5. By examining this figure one can easily check that any edge of the color code lattice Λ_t connects some site of Δ^0 and some site Δ^2 .

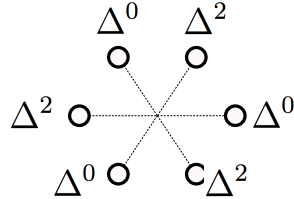


Figure 5: A local neighborhood of a site $\mathbf{j} \in \Delta^1$. This shows that any edge of the color code lattice $\Lambda_t = \Delta^0 \cup \Delta^2$ has one endpoint in Δ^0 and the other endpoint in Δ^2 .

It follows that $|f^i \cap \Delta^0| - |f^i \cap \Delta^2| = 3 - 3 = 0$ for hexagonal faces f^i and $|f^i \cap \Delta^0| - |f^i \cap \Delta^2| = 2 - 2 = 0$ for square faces f^i . Likewise, consider any pair of faces f^i, f^j such that $f^i \cap f^j \neq \emptyset$. Then $f^i \cap f^j$ is an edge of the color code lattice Λ_t , so that

$$|f^i \cap f^j \cap \Delta^0| - |f^i \cap f^j \cap \Delta^2| = 1 - 1 = 0.$$

This proves that all terms in Eq. (57) are zero, that is, \mathcal{S} is triply-even as promised. □

Finally, let ω_t^1, ω_t^2 and ω_t^3 be the vectors supported on the right, on the left, and on the bottom sides of the triangle that forms the boundary of Λ_t . In other words,

$$\omega_t^i = \{\mathbf{j} \in \Lambda_t : j_i = 0\}, \quad i = 1, 2, 3. \quad (58)$$

Note that ω_t^i are logical operators, that is, $\omega_t^i \in \mathcal{S}_t^\perp \cap \mathcal{O}$. Furthermore, $|\omega_t^i| = 2t + 1 \equiv d$, that is, ω_t^i are minimum weight logical operators.

10 Doubling transformation

Let us now describe a general construction of triply even subspaces inspired by Ref. [20]. Consider a pair of integers m, n and a pair of subspaces

$$\mathcal{S} \subseteq \mathbb{F}_2^m \quad \text{and} \quad \mathcal{T} \subseteq \mathbb{F}_2^n.$$

Let $k = 2m + n$. Partition the set of integers $[k]$ into three consecutive blocks, $[k] = ABC$, such that $|A| = |B| = m$ and $|C| = n$. Define a subspace $\mathcal{U} \subseteq \mathbb{F}_2^k$ such that

$$\mathcal{U} = \langle f[A] + f[B] : f \in \mathcal{S} \rangle + \mathcal{T}[C] + \langle BC \rangle. \quad (59)$$

Here we used a shorthand notation $BC \equiv \bar{1}[BC]$. This definition can be rephrased in terms of the generating matrices of \mathcal{S} and \mathcal{T} . Recall that S is a generating matrix of a linear subspace \mathcal{S} if \mathcal{S} is spanned by rows of S . Suppose \mathcal{S} and \mathcal{T} have generating matrices S and T respectively. Then \mathcal{U} has a generating matrix

$$U = \begin{bmatrix} S & S & & \\ & & T & \\ & \bar{1} & & \bar{1} \end{bmatrix} \quad (60)$$

where the three groups of columns correspond to A, B , and C respectively. Here we only show the non-zero entries of U . The mapping from \mathcal{S} and \mathcal{T} to \mathcal{U} will be referred to as a doubling map since it involves taking two copies of \mathcal{S} . We shall use an informal notation $\mathcal{U} = 2\mathcal{S} + \mathcal{T}$ to indicate that \mathcal{U} is obtained from \mathcal{S} and \mathcal{T} via the doubling map as described above.

Given a subset $M \subseteq [m]$ and a subset $N \subseteq [n]$ let $MMN \subseteq ABC$ be a subset obtained by choosing the subset M in the blocks A, B and choosing the subset N in the block C .

Lemma 2. *Assume \mathcal{S} is doubly even with respect to some subsets $M^\pm \subseteq [m]$ and \mathcal{T} is triply even with respect to some subsets $N^\pm \subseteq [n]$ such that*

$$|M^+| - |M^-| + |N^-| - |N^+| = 0 \pmod{8}. \quad (61)$$

Then $\mathcal{U} = 2\mathcal{S} + \mathcal{T}$ is triply even with respect to subsets $K^\pm = M^\pm M^\mp N^\mp$.

Proof. Consider first a vector

$$h = f[A] + f[B] + g[C] \in \mathcal{U},$$

where $f \in \mathcal{S}$ and $g \in \mathcal{T}$. By assumption,

$$|f \cap M^+| - |f \cap M^-| = 0 \pmod{4} \quad \text{and} \quad |g \cap N^+| - |g \cap N^-| = 0 \pmod{8}. \quad (62)$$

The identity $|h \cap K^\pm| = 2|f \cap M^\pm| + |g \cap N^\mp|$ then implies

$$|h \cap K^+| - |h \cap K^-| = 0 \pmod{8}.$$

Consider now a vector

$$h' = h + BC \in \mathcal{U}.$$

Then

$$|h' \cap K^\pm| = |f \cap M^\pm| + (|M^\pm| - |f \cap M^\pm|) + (|N^\mp| - |g \cap N^\mp|) = |M^\pm| + |N^\mp| - |g \cap N^\mp|.$$

Taking into account Eqs. (61,62) one arrives at

$$|h' \cap K^+| - |h' \cap K^-| = 0 \pmod{8}.$$

Since any vector of \mathcal{U} can be written as h or h' , the lemma is proved. \square

Next let us compute the orthogonal subspace \mathcal{U}^\perp . We specialize to the case when m, n are odd, whereas all vectors in \mathcal{S} and \mathcal{T} have even weight. This will be the case for applications considered below, where \mathcal{S} and \mathcal{T} define stabilizer groups of CSS-type quantum codes.

Lemma 3. *Suppose n and m are odd. Suppose $\mathcal{S} \subseteq \mathcal{E}$ and $\mathcal{T} \subseteq \mathcal{E}$. Then*

$$\mathcal{U}^\perp = \langle f[A] + f[B] : f \in \mathcal{E} \rangle + \mathcal{S}^\perp[A] + \dot{\mathcal{T}}[C] + \langle BC \rangle. \quad (63)$$

Furthermore,

$$\dot{\mathcal{U}} = \langle f[A] + f[B] : f \in \mathcal{E} \rangle + \dot{\mathcal{S}}[B] + \dot{\mathcal{T}}[C] + \langle BC \rangle. \quad (64)$$

and

$$d(\mathcal{U}) = \min \{d(\mathcal{S}), d(\mathcal{T}) + 2\}. \quad (65)$$

Proof. Consider an arbitrary vector $h \in \mathbb{F}_2^k$. By definition, the inclusion $h \in \mathcal{U}^\perp$ is equivalent to

$$h_A + h_B \in \mathcal{S}^\perp, \quad h_C \in \mathcal{T}^\perp, \quad \text{and} \quad h_B \oplus h_C \in \mathcal{E}. \quad (66)$$

A direct inspection shows that Eq. (66) holds if h belongs to each individual term in Eq. (63) which proves the inclusion \supseteq in Eq. (63). Conversely, suppose $h \in \mathcal{U}^\perp$. We have to prove that h is contained in the sum of the four terms in Eq. (63). Set $f = h_B$ if $h_B \in \mathcal{E}$ and $f = h_B + \bar{1}$ if $h_B \in \mathcal{O}$. In both cases $f \in \mathcal{E}$. Replacing h by $h + f[A] + f[B]$ we can make $h_B = \bar{0}$ or $h_B = \bar{1}$. Since $\bar{1} \in \mathcal{S}^\perp$, the first

condition in Eq. (66) implies $h_A \in \mathcal{S}^\perp$. If $h_B = \bar{1}$, replace h by $h + \bar{1}[B] + \bar{1}[C]$. This makes $h_B = \bar{0}$ and does not change the second condition in Eq. (66) since $\bar{1} \in \mathcal{T}^\perp$. The last condition in Eq. (66) then implies $h_C \in \mathcal{E}$. We conclude that $h = g[A] + g'[C]$ for some $g \in \mathcal{S}^\perp$ and $g' \in \dot{\mathcal{T}}$. This proves Eq. (63).

To prove Eq. (64) we note that odd-weight vectors in \mathcal{U}^\perp can only originate from the term $\mathcal{S}^\perp[A]$. Restriction to the even subspace replaces this term by $\dot{\mathcal{S}}[A]$. Since we already know that $\dot{\mathcal{U}}$ contains all vectors $f[A] + f[B]$ with $f \in \mathcal{E}$, we can move $\dot{\mathcal{S}}$ from A to B without changing $\dot{\mathcal{U}}$. This proves Eq. (64).

It remains to prove Eq. (65). Choose any vectors $f^* \in \mathcal{S}^\perp \cap \mathcal{O}$ and $g^* \in \mathcal{T}^\perp \cap \mathcal{O}$ such that $d(\mathcal{S}) = |f^*|$ and $d(\mathcal{T}) = |g^*|$. Choose any $i \in [m]$ and consider vectors $x = e^i[A] + e^i[B] + g^*[C]$ and $y = f^*[A]$. A direct inspection shows that $x, y \in \mathcal{U}^\perp \cap \mathcal{O}$. Therefore $d(\mathcal{U}) \leq |x| = 2 + |g^*| = d(\mathcal{T}) + 2$ and $d(\mathcal{U}) \leq |y| = |f^*| = d(\mathcal{S})$. This proves the inequality \leq in Eq. (65). Let us prove the reverse inequality. Consider any vector $h \in \mathcal{U}^\perp \cap \mathcal{O}$. It must satisfy Eq. (66). Since $h \in \mathcal{O}$, the condition $h_B \oplus h_C \in \mathcal{E}$ implies $h_A \in \mathcal{O}$. Consider two cases. Case 1: $h_C \in \mathcal{O}$. Then the second condition in Eq. (66) implies $h_C \in \mathcal{T}^\perp \cap \mathcal{O}$, that is, $|h_C| \geq d(\mathcal{T})$. Furthermore, since $h, h_C, h_A \in \mathcal{O}$ we infer that $h_B \in \mathcal{O}$ which implies $|h| = |h_A| + |h_B| + |h_C| \geq 2 + d(\mathcal{T})$. Case 2: $h_C \in \mathcal{E}$. Then the condition $h_B \oplus h_C \in \mathcal{E}$ implies $h_B \in \mathcal{E}$, that is, $h_A + h_B \in \mathcal{O}$. The first condition in Eq. (66) implies $h_A + h_B \in \mathcal{S}^\perp \cap \mathcal{O}$, that is, $|h_A + h_B| \geq d(\mathcal{S})$. By triangle inequality, $|h_A| + |h_B| \geq d(\mathcal{S})$ and thus $|h| \geq d(\mathcal{S})$. This proves the inequality \geq in Eq. (65). \square

The above lemma has the following obvious corollary.

Corollary 1. *Suppose n and m are odd, $\mathcal{S} \subseteq \mathcal{E}$, and \mathcal{T} is self-orthogonal. Then \mathcal{U} is self-orthogonal.*

Proof. Self-orthogonality of \mathcal{T} implies $\mathcal{T} \subseteq \dot{\mathcal{T}}$. Thus the first, the second, and the third terms of Eq. (59) are contained in the first, the third, and the fourth terms of Eq. (63) respectively. \square

11 Doubled color codes: construction

Let \mathcal{S}_t be the subspace spanned by faces of the color code lattice Λ_t constructed in Section 9. Recall that $\mathcal{S}_t \subseteq \mathbb{F}_2^{m_t}$ where $m_t \equiv |\Lambda_t| = 3t^2 + 3t + 1$. A doubled color code with distance $d = 2t + 1$ will require n_t physical qubits, where $n_0 = 1$ and

$$n_t = 2m_t + n_{t-1} \quad \text{for } t \geq 1. \quad (67)$$

Solving the recurrence relation gives

$$n_t = 2t^3 + 6t^2 + 6t + 1. \quad (68)$$

For instance, $n_1 = 15$, $n_2 = 53$, and $n_3 = 127$. Define a family of subspaces $\mathcal{T}_t \subseteq \mathbb{F}_2^{m_t}$ such that $\mathcal{T}_0 = \langle 0 \rangle \subseteq \mathbb{F}_2$ and

$$\mathcal{T}_t = 2\mathcal{S}_t + \mathcal{T}_{t-1}, \quad (69)$$

In other words, \mathcal{T}_t is obtained by applying the doubling map of Section 10 with $\mathcal{S} = \mathcal{S}_t$ and $\mathcal{T} = \mathcal{T}_{t-1}$. To describe this more explicitly, partition the set of integers $[n_t]$ into $2t + 1$ consecutive blocks as

$$[n_t] = A_t B_t \dots A_2 B_2 A_1 B_1 A_0 \quad \text{where} \quad A_r \cong B_r \cong \Lambda_r. \quad (70)$$

In other words, A_r and B_r represent two copies of the color code lattice Λ_r . Then

$$\mathcal{T}_t = \sum_{r=1}^t \langle f[A_r] + f[B_r] : f \in \mathcal{S}_r \rangle + \sum_{r=1}^t \langle B_r A_{r-1} \rangle. \quad (71)$$

We can also describe \mathcal{T}_t by its generating matrix. Suppose S_t is a generating matrix of \mathcal{S}_t such that rows of S_t correspond to faces of the color code lattice Λ_t . Then \mathcal{T}_t has a generating matrix

$$T_t = \begin{array}{|c|c|c|c|c|c|c|c|c|c|} \hline A_t & B_t & A_{t-1} & B_{t-1} & & & A_2 & B_2 & A_1 & B_1 & A_0 \\ \hline S_t & S_t & & & & & & & & & \\ \hline & & S_{t-1} & S_{t-1} & & & & & & & \\ \hline & & & & \dots & \dots & & & & & \\ \hline & & & & & & S_2 & S_2 & & & \\ \hline & \bar{1} & \bar{1} & & & & & & S_1 & S_1 & \\ \hline & & & \bar{1} & \bar{1} & & & & & & \\ \hline & & & & \dots & \dots & \bar{1} & & & & \\ \hline & & & & & & & \bar{1} & \bar{1} & & \\ \hline & & & & & & & & & \bar{1} & 1 \\ \hline \end{array}$$

Here the first line indicates which block of qubits contains a given group of columns. We shall use the subspace \mathcal{T}_t to construct the T -code as defined in Table 2. Let us prove that \mathcal{T}_t has the properties stated in Section 8.

Lemma 4. *The subspace \mathcal{T}_t is triply even with respect to some subsets $N_t^\pm \subseteq [n_t]$ satisfying*

$$|N_t^+| - |N_t^-| = 1. \quad (72)$$

Proof. We shall use induction in t . The base of induction, $t = 0$, corresponds to $n_0 = 1$ and $\mathcal{T}_0 = \langle 0 \rangle \subseteq \mathbb{F}_2$. Clearly, \mathcal{T}_0 is triply even with respect to subsets

$$N_0^+ = \{1\}, \quad N_0^- = \emptyset \quad (73)$$

which obey Eq. (72). Consider now an arbitrary t . We already know that \mathcal{S}_t is doubly even with respect to the subsets Δ_t^0 and Δ_t^2 such that

$$|\Delta_t^0| - |\Delta_t^2| = 1, \quad (74)$$

see Fact 1. Define

$$A_t^+ = B_t^+ = \Delta_t^0 \quad \text{and} \quad A_t^- = B_t^- = \Delta_t^2. \quad (75)$$

Here we consider A_t^\pm and B_t^\pm as subsets of A_t and B_t respectively. Choose

$$N_t^\pm = A_t^\pm B_t^\pm N_{t-1}^\mp, \quad t \geq 1. \quad (76)$$

Combining Eqs. (74,75,76) and assuming that $|N_{t-1}^+| - |N_{t-1}^-| = 1$ one gets

$$|N_t^+| - |N_t^-| = 2(|\Delta_t^2| - |\Delta_t^0|) + |N_{t-1}^-| - |N_{t-1}^+| = 1. \quad (77)$$

This proves Eq. (72) for all $t \geq 0$. Furthermore, Eqs. (72,74,75) imply

$$|A_t^+| - |A_t^-| - |N_t^+| + |N_t^-| = 0$$

for all $t \geq 0$. This shows that condition Eq. (61) of Lemma 2 is satisfied for $M^\pm = A_t^\pm = B_t^\pm$. The lemma implies that \mathcal{T}_t is triply even with respect to the subsets N_t^\pm for all $t \geq 0$. \square

Let us use induction in t to show that \mathcal{T}_t has distance

$$d(\mathcal{T}_t) = 2t + 1. \quad (78)$$

Indeed, $d(\mathcal{T}_0) = 1$ since $\mathcal{T}_0^\perp = \langle 0 \rangle^\perp = \mathbb{F}_2$ and the only odd-weight vector in \mathbb{F}_2 is 1. Furthermore, the color code on the lattice Λ_t has distance $2t + 1$, that is, $d(\mathcal{S}_t) = 2t + 1$, see Fact 1. Assuming that $d(\mathcal{T}_{t-1}) = 2t - 1$ and using Eq. (65) of Lemma 3 we infer that $d(\mathcal{T}_t) = \min \{d(\mathcal{S}_t), 2 + d(\mathcal{T}_{t-1})\} = 2t + 1$ which proves Eq. (78) for all $t \geq 0$.

To construct the T -code we shall also need a subspace $\dot{\mathcal{T}}_t$, see Table 2. It will be convenient to rewrite the partition in Eq. (70) as $[n_t] = A_t B_t C_t$, where

$$C_t = A_{t-1} B_{t-1} \dots A_1 B_1 A_0.$$

Applying Eq. (64) of Lemma 3 and taking into account that $\dot{\mathcal{S}}_t = \mathcal{S}_t$, see Fact 1, one gets $\dot{\mathcal{T}}_0 = 0$ and

$$\dot{\mathcal{T}}_t = \langle f[A_t] + f[B_t] : f \in \mathcal{E} \rangle + \mathcal{S}_t[B_t] + \dot{\mathcal{T}}_{t-1}[C_t] + \langle B_t A_{t-1} \rangle \quad (79)$$

for $t \geq 1$. Let $\omega_t \in \mathcal{S}_t^\perp \cap \mathcal{O}$ be some fixed minimum weight logical operator of the regular color code such that $|\omega_t| = 2t + 1$. Later on we shall choose ω_t as defined in Eq. (58). Then $\bar{1} = \omega_t + g$ for some $g \in \mathcal{S}_t$, see Eq. (54) of Fact 1. This implies $B_t A_{t-1} = \omega_t[B_t] + g[B_t] + A_{t-1}$. Since $g[B_t]$ is contained in the second term in Eq. (79), we can replace the last term by $\langle \omega_t[B_t] + A_{t-1} \rangle$. Likewise,

$$A_{t-1} = \omega_{t-1}[A_{t-1}] + f[C_t]$$

for some $f \in \dot{\mathcal{T}}_{t-1}$. Here we noted that both $\bar{1}[A_{t-1}]$ and $\omega_{t-1}[A_{t-1}]$ are contained in $\mathcal{T}_{t-1}^\perp \cap \mathcal{O}$, so that the sum of them is contained in $\mathcal{T}_{t-1}^\perp \cap \mathcal{E} \equiv \dot{\mathcal{T}}_{t-1}$. Since $f[C_t]$ is contained in the third term in Eq. (79), we can rewrite the last term as $\langle \omega_t[B_t] + \omega_{t-1}[A_{t-1}] \rangle$. Therefore

$$\dot{\mathcal{T}}_t = \langle f[A_t] + f[B_t] : f \in \mathcal{E} \rangle + \mathcal{S}_t[B_t] + \dot{\mathcal{T}}_{t-1}[C_t] + \langle \omega_t[B_t] + \omega_{t-1}[A_{t-1}] \rangle \quad (80)$$

for $t \geq 1$. Note that here we can add a term $\mathcal{S}_t[A_t]$ since $f[A_t] + f[B_t]$ is contained in the first term in Eq. (80) for any $f \in \mathcal{S}_t$. We can also describe $\dot{\mathcal{T}}_t$ by its generating matrix. Suppose E_t is a generating matrix of the even subspace \mathcal{E}^{m_t} such that rows of E_t correspond to edges of the color code lattice Λ_t , that is, each row of E_t has a form $e^u + e^v$ for some edge (u, v) of Λ_t . Then $\dot{\mathcal{T}}_t$ has a generating matrix

$$\dot{\mathcal{T}}_t = \begin{array}{|c|c|c|c|c|c|c|c|c|c|} \hline & A_t & B_t & A_{t-1} & B_{t-1} & & & A_2 & B_2 & A_1 & B_1 & A_0 \\ \hline S_t & & & & & & & & & & & \\ & S_t & & & & & & & & & & \\ & & S_{t-1} & & & & & & & & & \\ & & & S_{t-1} & & & & & & & & \\ & & & & \dots & \dots & & & & & & \\ & & & & & & S_2 & & & & & \\ & & & & & & & S_2 & & & & \\ & & & & & & & & S_1 & & & \\ E_t & E_t & & & & & & & & S_1 & & \\ & & E_{t-1} & E_{t-1} & & & & & & & & \\ & & & & \dots & \dots & & & & & & \\ & & & & & & E_2 & E_2 & & & & \\ & & & & & & & & E_1 & E_1 & & \\ & & \omega_t & & & & & & & & & \\ & & & \omega_{t-1} & & & & & & & & \\ & & & & \omega_{t-1} & & & & & & & \\ & & & & & \omega_{t-2} & & & & & & \\ & & & & & \dots & \dots & & & & & \\ & & & & & & \omega_3 & & & & & \\ & & & & & & & \omega_2 & & & & \\ & & & & & & & & \omega_2 & & & \\ & & & & & & & & & \omega_1 & & \\ & & & & & & & & & & \omega_1 & \\ & & & & & & & & & & & 1 \\ \hline \end{array}$$

We shall refer to the first two groups of rows as *face-type* generators and *edge-type* generators.

To construct the C -code we shall need a subspace $\mathcal{C}_t \subseteq \mathbb{F}_2^{n_t}$ defined as

$$\mathcal{C}_t = \sum_{r=1}^t \langle f[A_r] + g[B_r] : f, g \in \mathcal{S}_r \rangle + \sum_{r=1}^t \langle B_r A_{r-1} \rangle. \quad (81)$$

By comparing Eqs. (71,79,81) one can see that

$$\mathcal{T}_t \subseteq \mathcal{C}_t = \dot{\mathcal{C}}_t \subseteq \dot{\mathcal{T}}_t. \quad (82)$$

A generating matrix of \mathcal{C}_t can be obtained from $\dot{\mathcal{T}}_t$ by removing all edge-type generators. A direct inspection shows that generators of \mathcal{C}_t can be partitioned into mutually disjoint subsets supported on regions

$$M_t = A_t, \quad M_{t-1} = B_t A_{t-1}, \quad M_{t-2} = B_{t-1} A_{t-2}, \quad \dots, \quad M_0 = B_1 A_0.$$

Thus we can analyze properties of \mathcal{C}_t on each region M_r separately. Generators of \mathcal{C}_t supported on M_t have a form $f[A_t]$ with $f \in \mathcal{S}_t$. These generators describe the regular color code \mathcal{S}_t . Generators supported on a region M_r describe the two-qubit EPR state $|0,0\rangle + |1,1\rangle$ shared between B_{r+1} and A_r such that the two qubits are encoded by the regular color code \mathcal{S}_{r+1} and \mathcal{S}_r . As a consequence we obtain

Corollary 2. *The subspace \mathcal{C}_t is doubly even with respect to the subsets $\Delta_t^{0,2} \subseteq A_t$, see Fact 1. Furthermore, $d(\mathcal{C}_t) = 2t + 1$.*

At this point we have proved all properties of the subspaces $\mathcal{C}_t, \mathcal{T}_t$ stated in Section 8 except for the spatial locality. Let Λ be the honeycomb lattice with two qubits per site. We shall allocate a triangular-shaped region of Λ isomorphic to the color code lattice Λ_t to accommodate the blocks of qubits A_t and B_t . The two blocks can share the same set of sites since each site contains two qubits. By a slight abuse of terminology, we shall identify Λ_t and the region of Λ accommodating A_t and B_t . The regions Λ_t and Λ_{t-1} are placed next to each other as shown on Fig. 6.

Consider the generating matrix \dot{T}_t defined above. We shall say that a vector $f \in \mathbb{F}_2^{n_t}$ is *spatially local* if its support is contained in a single face of the lattice. By definition, face-type and edge-type generators of \dot{T}_t are spatially local. Consider some row of \dot{T}_t in the bottom group. It has a form

$$\omega_{r,r-1} \equiv \omega_r[B_r] + \omega_{r-1}[A_{r-1}], \quad r = 1, \dots, t.$$

The above arguments show that we are free to choose different logical operators ω_r in different generators $\omega_{r,r-1}$. Let us use this freedom to choose

$$\omega_{r,r-1} \equiv \omega_r^i[B_r] + \omega_{r-1}^j[A_{r-1}] \tag{83}$$

where ω_r^i is the minimum weight logical operator supported on the i -th boundary of the lattice Λ_r , see Eq. (58). Furthermore, we can choose i and j such that the i -th boundary of Λ_r is located next to the j -th boundary of Λ_{r-1} , see Fig. 6. Then the generator $\omega_{r,r-1}$ has a shape of a loop that encloses the free space separating the regions Λ_r and Λ_{r-1} . Since $|\omega_r^i| = 2r+1$, we get $|\omega_{r,r-1}| = 2r+1+2r-1 = 4r$. We shall explain how to reduce the weight of the generators $\omega_{r,r-1}$ and make them spatially local in the next section.

The above discussion also shows that a code deformation transforming the C -code to the T -code requires only spatially local syndrome measurements. Indeed, suppose ρ_L is some logical state of the C -code, see Table 2. One can first apply a reverse gauge fixing that extends the gauge group of ρ_L from $\text{CSS}(\mathcal{C}_t, \mathcal{C}_t)$ to $\text{CSS}(\mathcal{C}_t, \dot{\mathcal{T}}_t)$. This can be achieved by applying a random element of the group $Z(\dot{\mathcal{T}}_t)$. This also restricts the stabilizer group of ρ_L from $\text{CSS}(\mathcal{C}_t, \mathcal{C}_t)$ to $\text{CSS}(\mathcal{T}_t, \mathcal{C}_t)$. We note that

$$\dot{\mathcal{T}}_t = \mathcal{C}_t + \sum_{l=(u,v)} \langle l[A] + l[B] \rangle,$$

where the sum runs over all edges of the sub-lattices $\Lambda_1, \dots, \Lambda_r$. Thus a gauge fixing that extends the stabilizer group of ρ_L from $\text{CSS}(\mathcal{T}_t, \mathcal{C}_t)$ to $\text{CSS}(\mathcal{T}_t, \dot{\mathcal{T}}_t)$ can be realized by measuring syndromes of the edge-type stabilizers $Z(l[A] + l[B])$ and applying a suitable recovery operator.

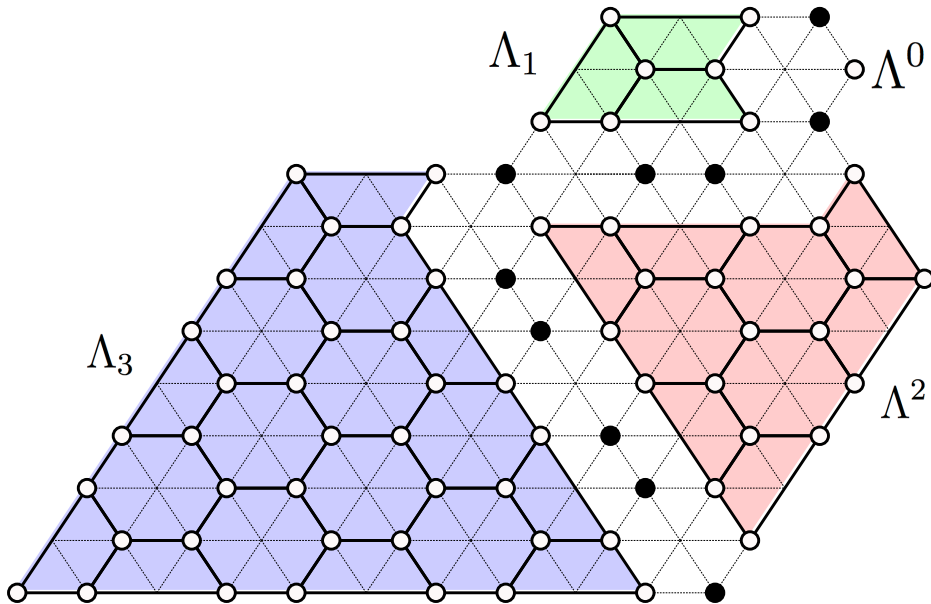


Figure 6: Embedding of the doubled color code \mathcal{T}_3 into the hexagonal lattice Λ with two qubits per site. The lattice is divided into four disjoint regions $\Lambda_0, \Lambda_1, \Lambda_2, \Lambda_3$ where Λ_t accommodates two copies of the color code \mathcal{S}_t labeled A_t and B_t (not shown). Recall that Λ_0 is a single site. To enable a more regular embedding we twisted one corner of each lattice Λ_t compared with Fig. 4. Sites represented by solid circles can be ignored at this point. To obtain the next code \mathcal{T}_4 one should attach Λ_4 to the bottom side of Λ_3 . To obtain \mathcal{T}_5 one should attach Λ_5 to the left side of Λ_4 . The process continues in the alternating fashion. Gauge generators live on edges and faces of the lattice. There are also non-local gauge generators $\omega_{t,t-1}$ of weight $4t$ connecting B -qubits on the boundary of Λ_t and A -qubits on the boundary of Λ_{t-1} (not shown).

12 Weight reduction

In this section we transform the C -code into a local form. This requires two steps. First, we show how to represent each non-local gauge generator $\omega_{r,r-1}$, see Eq. (83), as a sum of spatially local generators of weight at most six and a single non-local generator of weight two. Secondly, we show how to represent each of the remaining non-local generators as a sum of spatially local generators of weight two. Each of these steps extends the code by adding several ancillary qubits and gauge generators. We add the same ancillary qubits and gauge generators to both C and T codes to preserve the local mapping between them. Accordingly, we have to prove that the extended versions of the C and T codes have the same distance and the same transversality properties as the original codes.

We begin by setting up some notations. Below we consider some fixed value of t and $r = 1, \dots, t$. Let us denote the sites of Λ_r lying on the boundary facing Λ_{r-1} as $u^1, u^2, \dots, u^{2r+1}$. The ordering is chosen such that u^{2r+1} is the “twisted” corner of Λ_r , see Fig. 7. Let us denote the sites of Λ_{r-1} lying on the boundary facing Λ_r as $v^1, v^2, \dots, v^{2r-1}$. The ordering is chosen such that u^i and v^i are

next-to-nearest neighbors, see Fig. 7. Using these notations one can rewrite Eq. (83) as

$$\omega_{r,r-1} = \sum_{i=1}^{2r+1} u^i [B_r] + \sum_{i=1}^{2r-1} v^i [A_{r-1}]. \quad (84)$$

Consider now sites of Λ lying in the free space separating Λ_r and Λ_{r-1} . These sites are indicated by filled circles on Figs. 6,7. Denote these sites as w^1, w^2, \dots, w^{2r} , see Fig. 7, and let

$$D_r = \{w^1, \dots, w^{2r}\}.$$

The ordering is chosen such that w^i is a nearest neighbor of u^i and v^i for all $1 \leq i \leq 2r - 1$. Furthermore, w^{2i} is a nearest neighbor of w^{2i+1} .

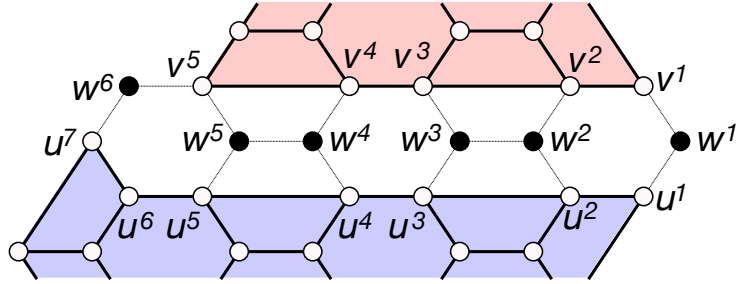


Figure 7: Sites u^i on the boundary of Λ_3 (blue), sites v^i on the boundary of Λ_2 (red), and sites w^i in the region D_3 (filled circles). The lattice is rotated 60° counter-clockwise compared with Fig. 6.

Let us add $2r$ ancillary qubits such that each site of D_r contains one qubit. The total number of physical qubits in the lattice Λ becomes

$$N_t = n_t + \sum_{r=1}^t 2r = 2t^3 + 7t^2 + 7t + 1, \quad (85)$$

see Eq. (68). Accordingly, the partition Eq. (70) becomes

$$[N_t] = A_t B_t D_t \dots A_2 B_2 D_2 A_1 B_1 D_1 A_0. \quad (86)$$

We shall use terms A -qubit, B -qubit, and D -qubit to indicate which of the blocks in Eq. (86) contains a given qubit. Note that the site w^{2r} of D_r and the site w^1 of D_{r-1} coincide, see Fig. 6. However, since we placed only one qubit at w^{2r} and w^1 , the total number of qubits per site is at most two.

For each $r = 1, \dots, t$ define $2r$ additional gauge generators g_r^i and h_r^i with $i = 1, \dots, r$ as shown below, see also Fig. 8.

$$g_r^i = (w^{2i} + w^{2i+1})[D_r], \quad (87)$$

where $i = 1, \dots, r - 1$,

$$g_r^r = (w^1 + w^{2r})[D_r], \quad (88)$$

$$h_r^i = (w^{2i-1} + w^{2i})[D_r] + (u^{2i-1} + u^{2i})[B_r] + (v^{2i-1} + v^{2i})[A_{r-1}], \quad (89)$$

where $i = 1, \dots, r-1$, and

$$h_r^r = (w^{2r-1} + w^{2r})[D_r] + (u^{2r-1} + u^{2r} + u^{2r+1})[B_r] + v^{2r-1}[A_{r-1}]. \quad (90)$$

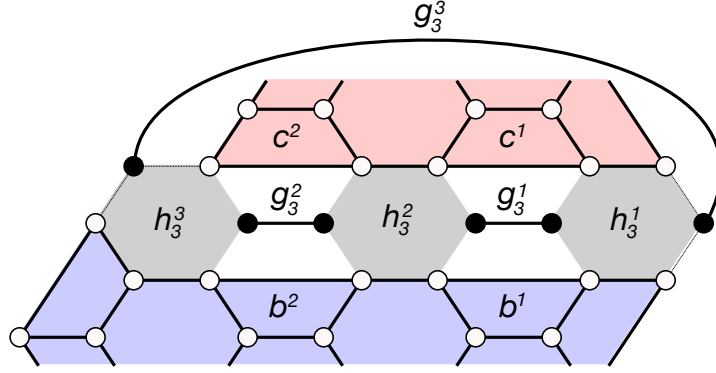


Figure 8: Additional gauge generators h_r^i and g_r^i for $r = 3$. The generator h_r^i acts on B -qubits at the boundary of Λ_r (blue) and A -qubits at the boundary of Λ_{r-1} (red). In addition, h_r^i acts on two D -qubits (filled circles). The generator g_r^i acts only on two D -qubits. The special faces b^i and c^i of the color code lattice are used to define modified stabilizers. The original stabilizer $b^i[A_r] + b^i[B_r] \in \mathcal{T}_t$ must be replaced by $g_r^i + b^i[A_r] + b^i[B_r] \in \mathcal{U}_t$. The original stabilizer $c^i[A_r] + c^i[B_r] \in \mathcal{T}_t$ must be replaced by $g_{r+1}^i + c^i[A_r] + c^i[B_r] \in \mathcal{U}_t$.

Note that all additional generators except for g_r^r are spatially local. Furthermore,

$$\omega_{r,r-1} = \sum_{i=1}^r h_r^i + g_r^i. \quad (91)$$

This identity will allow us to get rid of the non-local generators $\omega_{r,r-1}$. More formally, define a subspace $\mathcal{U}_t \subseteq \mathcal{E}^{N_t}$ such that

$$\dot{\mathcal{U}}_t = \dot{\mathcal{T}}_t + \sum_{r=1}^t \langle g_r^1, \dots, g_r^r, h_r^1, \dots, h_r^r \rangle. \quad (92)$$

Note that $\dot{\mathcal{U}}_t$ uniquely defines \mathcal{U}_t since applying the dot operation twice gives the original subspace, see Section 3. We shall see that \mathcal{U}_t can be regarded as an extended version of \mathcal{T}_t . Similarly, define a subspace $\mathcal{D}_t \subseteq \mathcal{E}^{N_t}$ such that

$$\dot{\mathcal{D}}_t = \dot{\mathcal{C}}_t + \sum_{r=1}^t \langle g_r^1, \dots, g_r^r, h_r^1, \dots, h_r^r \rangle. \quad (93)$$

We shall see that \mathcal{D}_t can be regarded as an extended version of \mathcal{C}_t . Here it is understood that vectors from $\dot{\mathcal{T}}_t$ and $\dot{\mathcal{C}}_t$ are extended to D -qubits by zeros. From Eq. (82) we infer that

$$\dot{\mathcal{D}}_t \subseteq \dot{\mathcal{U}}_t \quad \text{and} \quad \mathcal{U}_t \subseteq \mathcal{D}_t. \quad (94)$$

Let us establish some basic properties of \mathcal{D}_t and \mathcal{U}_t .

Lemma 5. $\mathcal{U}_t \subseteq \dot{\mathcal{U}}_t$. Furthermore, if $h \in \mathcal{U}_t$ then the restriction of h onto the union of A and B qubits is contained in \mathcal{T}_t .

Lemma 6. $\mathcal{D}_t \subseteq \dot{\mathcal{D}}_t$. Furthermore, if $h \in \mathcal{D}_t$ then the restriction of h onto the union of A and B qubits is contained in \mathcal{C}_t .

Since the proof of the two lemmas is identical, we only prove Lemma 5.

Proof. Suppose $h \in \mathcal{U}_t$. By definition of the dot operation, h has even weight and orthogonal to any vector of $\dot{\mathcal{U}}_t$. Let h_D be a restriction of h onto the union of all D -qubits. Since h_D is orthogonal to any generator g_r^i , we infer that h_D is a linear combination of g_r^i . This implies $h_D \in \dot{\mathcal{U}}_t$. Let h_{AB} be a restriction of h onto the union of all A - and B -qubits. Since $h \in \mathcal{E}$ and $h_D \in \mathcal{E}$, we infer that $h_{AB} \in \mathcal{E}$. The inclusion $\dot{\mathcal{T}}_t \subseteq \dot{\mathcal{U}}_t$ implies $h_{AB} \in \dot{\mathcal{T}}_t^\perp \cap \mathcal{E} = \mathcal{T}_t$. This proves the second statement. Finally, $\mathcal{T}_t \subseteq \dot{\mathcal{T}}_t \subseteq \dot{\mathcal{U}}_t$ implies $h_{AB} \in \mathcal{U}_t$, that is, $h \in \dot{\mathcal{U}}_t$. \square

Combining the lemmas and Eq. (94) yields

$$\mathcal{U}_t \subseteq \mathcal{D}_t \subseteq \dot{\mathcal{D}}_t \subseteq \dot{\mathcal{U}}_t. \quad (95)$$

One can view Eq. (95) as an extended version of Eq. (82). We can now define extended versions of the doubled color codes, see Table 3.

	Transversal gates	Stabilizer group	Gauge group
C -code	Clifford group	$\text{CSS}(\mathcal{D}_t, \mathcal{D}_t)$	$\text{CSS}(\dot{\mathcal{D}}_t, \dot{\mathcal{D}}_t)$
T -code	T gate	$\text{CSS}(\mathcal{U}_t, \dot{\mathcal{U}}_t)$	$\text{CSS}(\mathcal{U}_t, \dot{\mathcal{U}}_t)$
Base code		$\text{CSS}(\mathcal{U}_t, \mathcal{D}_t)$	$\text{CSS}(\dot{\mathcal{D}}_t, \dot{\mathcal{U}}_t)$

Table 3: Extended doubled color codes.

As before, we define the base code such that its stabilizer group is the intersection of stabilizer groups of all codes in the family. Lemma 6 implies that \mathcal{D}_t is self-orthogonal, that is, the group $\text{CSS}(\mathcal{D}_t, \mathcal{D}_t)$ is abelian and the C -code is well-defined. Likewise, Eq. (95) implies that \mathcal{U}_t and \mathcal{D}_t are mutually orthogonal, so that the group $\text{CSS}(\mathcal{U}_t, \mathcal{D}_t)$ is abelian and the base code is well-defined. Since we already know that \mathcal{C}_t is doubly even and \mathcal{T}_t is triply even, Lemmas 5,6 have the following corollary.

Corollary 3. *The subspace \mathcal{U}_t is triply even with respect to the same subsets as \mathcal{T}_t . The subspace \mathcal{D}_t is doubly even with respect to the same subsets as \mathcal{C}_t .*

This shows that the extended C and T codes have transversal Clifford gates and the T -gate respectively. Let us describe gauge generators of the extended C -code. From Eq. (91) we infer that the non-local generators $\omega_{r,r-1}$ can be removed from the generating set of $\dot{\mathcal{D}}_t$. Thus the extended C -code has only face-type gauge generators and the additional generators $g_r^1, \dots, g_r^r, h_r^1, \dots, h_r^r$. The latter are spatially local except for g_r^r . A direct inspection of Eq. (93) shows that generators of $\dot{\mathcal{D}}_t$ can be partitioned into mutually disjoint subsets supported on regions

$$M_t = A_t, \quad M_{t-1} = B_t D_t A_{t-1}, \quad M_{t-2} = B_{t-1} D_{t-1} A_{t-2}, \quad \dots, \quad M_0 = B_1 D_1 A_0.$$

Thus we can analyze properties of the extended C -code on each region M_r separately. Generators of $\dot{\mathcal{D}}_t$ supported on M_t have a form $f[A_t]$ with $f \in \mathcal{S}_t$. These generators describe the regular color code \mathcal{S}_t . Thus the extended C -code can be converted to the regular color code $\text{CSS}(\mathcal{S}_t, \mathcal{S}_t)$ by discarding all the regions except for M_t . As before, the extended T -code is obtained from the extended C -code by adding edge-type Z -stabilizers.

Next let us prove that the extended codes have distance $2t + 1$. Combining Eq. (7) and Eq. (95) one can see that the distance of any code defined in Table 3 is lower bounded by $d(\mathcal{U}_t)$. Thus it suffices to prove that $d(\mathcal{U}_t) = 2t + 1$. We shall need an explicit expression for generators of \mathcal{U}_t . Note that

$$g_r \equiv \sum_{i=1}^r g_r^i \in \mathcal{U}_t. \quad (96)$$

Indeed, g_r does not overlap with generators of $\dot{\mathcal{T}}_t$ and has even overlap with all additional generators g_r^i and h_r^i . Next consider a generator g_r^i with $1 \leq i < r$. Let $b^i \in \mathcal{S}_r$ be the face of Λ_r located directly below g_r^i , see Fig. 8. We claim that

$$\beta_r^i \equiv g_r^i + b^i[A_r] + b^i[B_r] \in \mathcal{U}_t \quad (97)$$

for all $r = 1, \dots, t$ and all $i = 1, \dots, r - 1$. Indeed, β_r^i has even overlap with all generators of $\dot{\mathcal{T}}_t$ since $b^i[A_r] + b^i[B_r] \in \mathcal{T}_t$. Furthermore, β_r^i has even overlap with all additional generators $g_r^{i'}$. It remains to check that β_r^i has even overlap with the additional generators h_r^j . The only non-trivial case is h_r^j with $j = i$ or $j = i + 1$, see Fig. 8. In this case both g_r^i and $b^i[A_r] + b^i[B_r]$ have odd overlap with h_r^j , so that β_r^i has even overlap with h_r^j . This proves that $\beta_r^i \in \mathcal{U}_t$.

Likewise, let $c^i \in \mathcal{S}_{t-1}$ be the face of Λ_{r-1} located directly above g_r^i , see Fig. 8. The same arguments as above show that

$$\gamma_r^i \equiv g_r^i + c^i[A_{r-1}] + c^i[B_{r-1}] \in \mathcal{U}_t \quad (98)$$

for all $r = 2, \dots, t$ and for all $i = 1, \dots, r - 1$. Note that the sublattice Λ_t has only special faces b^i whereas Λ_1 has only special faces c^i . All other sublattices Λ_r have both types of special faces. Now we are ready to describe generators of \mathcal{U}_t .

Lemma 7. Suppose $2 \leq r \leq t-1$. Let $\mathcal{S}_r^* \subseteq \mathcal{S}_r$ be the subspace spanned by all faces of the color code lattice Λ_r except for the special faces b^i and c^i . Let $\mathcal{S}_t^* \subseteq \mathcal{S}_t$ be the subspace spanned by all faces of Λ_t except for b^i . Let $\mathcal{S}_1^* \subseteq \mathcal{S}_1$ be the subspace spanned by all faces of Λ_1 except for c^1 . Then

$$\begin{aligned} \mathcal{U}_t = & \sum_{r=1}^t \langle f[A_r] + f[B_r] : f \in \mathcal{S}_r^* \rangle + \langle B_r A_{r-1} \rangle \\ & + \sum_{r=1}^t \langle g_r \rangle + \langle \beta_r^i, \gamma_r^i : i = 1, \dots, r-1 \rangle. \end{aligned} \quad (99)$$

Proof. We have already shown that the last two terms in Eq. (99) are contained in \mathcal{U}_t . A direct inspection shows that vectors $f[A_r] + f[B_r]$ with $f \in \mathcal{S}_r^*$ and $B_r A_{r-1}$ have even overlap with all additional generators g_j^i, h_j^i . Furthermore, $f[A_r] + f[B_r]$ and $B_r A_{r-1}$ are contained in \mathcal{T}_t and thus have even overlap with any vector in \mathcal{T}_t . This proves the inclusion \supseteq in Eq. (99).

Conversely, consider any $k \in \mathcal{U}_t$. We have to prove that k is contained in the righthand side of Eq. (99). The same arguments as in the proof of Lemma 5 show that

$$k = k_{AB} + k_D, \quad k_{AB} \in \mathcal{T}_t, \quad k_D = \sum_{r=1}^t \sum_{i=1}^r x_r^i g_r^i, \quad (100)$$

where k_{AB} and k_D have support only on AB -qubits and D -qubits respectively. Here $x_r^i \in \mathbb{F}_2$ are some coefficients. Let us modify k according to

$$k \leftarrow k + \sum_{r=1}^t \sum_{i=1}^r x_r^i \beta_r^i.$$

We still have the inclusion $k \in \mathcal{U}_k$ since $\beta_r^i \in \mathcal{U}_k$, see above. Furthermore, the term $x_r^i \beta_r^i$ cancels the term $x_r^i g_r^i$ in k_D and modifies the term k_{AB} according to $k_{AB} \leftarrow k_{AB} + b^i[A_r] + b^i[B_r]$. Now k has support only on AB -qubits and $k \in \mathcal{T}_t$. Let us express k as a sum of generators of \mathcal{T}_t defined in Eq. (71). This yields

$$k = k^* + \sum_{r=2}^t \sum_{i=1}^{r-1} y_r^i (b^i[A_r] + b^i[B_r]) + z_r^i (c^i[A_{r-1}] + c^i[B_{r-1}])$$

for some

$$k^* \in \sum_{r=1}^t \langle f[A_r] + f[B_r] : f \in \mathcal{S}_r^* \rangle + \langle B_r A_{r-1} \rangle$$

and some coefficients $y_r^i, z_r^i \in \mathbb{F}_2$. Note that k^* is contained in the righthand side of Eq. (99). Furthermore, $k^* \in \mathcal{U}_t$ which implies $k + k^* \in \mathcal{U}_t$. In particular, $k + k^*$ has even overlap with all generators h_r^j . On the other hand, h_r^j has odd overlap with $b^i[A_r] + b^i[B_r]$ and with $c^i[A_{r-1}] + c^i[B_{r-1}]$

for $i = j, j - 1$, see Fig. 8. Thus $k + k^*$ may have even overlap with h_r^j only if $y_r^i = z_r^i$ for all i and r . Using the identity

$$(b^i[A_r] + b^i[B_r]) + (c^i[A_{r-1}] + c^i[B_{r-1}]) = \beta_r^i + \gamma_r^i$$

we conclude that $k + k^*$ is contained in the last term in Eq. (99). Since k^* is contained in the sum of the first two terms in Eq. (99), we have proved the inclusion \subseteq in Eq. (99). \square

The following lemma is the most difficult part of the proof.

Lemma 8. $d(\mathcal{U}_t) = d(\mathcal{T}_t) = 2t + 1$.

Proof. We shall use induction in t . The base of induction is $t = 1$. In this case there are only two D -qubits, $D_1 = \{w^1, w^2\}$, and one additional gauge generator $g_1 \equiv g_1^1 = w^1 + w^2$. Furthermore, g_1 is a stabilizer, $g_1 \in \mathcal{U}_1$. Consider a minimum weight vector $k \in \mathcal{U}_1^\perp \cap \mathcal{O}$ such that $d(\mathcal{U}_1) = |k|$. Since k has even overlap with g_1 , one has either $g_1 \subseteq k$ or $g_1 \cap k = \emptyset$. The first case can be ruled out since $k + g_1 \in \mathcal{U}_1^\perp \cap \mathcal{O}$ would have weight $|k| - 2$. Thus k has support only on AB -qubits. Lemma 5 implies that \mathcal{U}_1 and \mathcal{T}_1 have the same restriction on AB -qubits, that is, $d(\mathcal{U}_1) = d(\mathcal{T}_1) = 3$.

Consider now some $t \geq 2$. Let us rewrite the partition in Eq. (86) as

$$[N_t] = A_t B_t D_t C_t, \quad C_t \equiv A_{t-1} B_{t-1} D_{t-1} \dots A_1 B_1 D_1 A_0.$$

Consider an arbitrary vector $k \in \mathcal{U}_t^\perp \cap \mathcal{O}$. Let us write

$$k = \alpha[A_t] + \beta[B_t] + \delta[D_t] + \gamma[C_t],$$

for some vectors

$$\alpha, \beta \in \mathbb{F}_2^{mt}, \quad \delta \in \mathbb{F}_2^{2t}, \quad \gamma \in \mathbb{F}_2^{N_{t-1}}.$$

First we claim that

$$\alpha \in \mathcal{O}, \quad \beta + \gamma \in \mathcal{E}, \quad \text{and} \quad \delta \in \mathcal{E}. \quad (101)$$

Indeed, since k has even overlap with the stabilizer g_t with $\text{supp}(g_t) = D_t$, see Eq. (96), we infer that $0 = k^\top g_t = |\delta| \pmod{2}$, that is, $\delta \in \mathcal{E}$. Furthermore, Lemma 7 implies

$$h \equiv B_t C_t = \sum_{r=1}^t B_r A_{r-1} + \sum_{r=1}^{t-1} g_r \in \mathcal{U}_t.$$

Since $\text{supp}(h) = B_t C_t$ and $0 = k^\top h = |\beta| + |\gamma| \pmod{2}$, we infer that $\beta + \gamma \in \mathcal{E}$. Finally, $\alpha \in \mathcal{O}$ follows from the above and the assumption that $k \in \mathcal{O}$.

We shall refer to a substitution $k \leftarrow k + g$ with $g \in \mathcal{U}_t$ as a gauge transformation. Note that gauge transformations preserve the set $\mathcal{U}_t^\perp \cap \mathcal{O}$. Our strategy will be to choose a sequence of gauge transformations that transform k into a form

$$k = e^i[A_t] + e^i[B_t] + \gamma[C_t] \quad (102)$$

without increasing the weight of k . Here e^i is some basis vector of $\mathbb{F}_2^{m_t}$. Let us first assume that k has the desired form Eq. (102) and show that this implies $|k| \geq 2t + 1$. Indeed, using Eq. (99) one can check that $e^i[A_t] + e^i[B_t]$ is orthogonal to all generators of \mathcal{U}_t except for $B_t A_{t-1}$. Therefore if $k \in \mathcal{U}_t^\perp$ has a special form Eq. (102) then $\gamma \in \mathcal{U}_{t-1}^\perp$. Furthermore, $k \in \mathcal{O}$ implies $\gamma \in \mathcal{O}$, that is, $\gamma \in \mathcal{U}_{t-1}^\perp \cap \mathcal{O}$. By induction hypothesis, $|\gamma| \geq 2t - 1$ and thus $|k| \geq 2t + 1$.

It remains to show that k can be transformed into the desired form Eq. (102) without increasing the weight. First, choose any $i \in \text{supp}(\alpha)$ and let $\alpha' = \alpha + e^i$. Note that $\alpha' \in \mathcal{E}$ due to Eq. (101), so that $\alpha'[A_t] + \alpha'[B_t] \in \dot{\mathcal{U}}_t$. In addition, $|\alpha'| = |\alpha| - 1$, so that

$$|k + \alpha'[A_t] + \alpha'[B_t]| = 1 + |\beta + \alpha'| + |\gamma| + |\delta| \leq 1 + |\alpha'| + |\beta| + |\gamma| + |\delta| = |\alpha| + |\beta| + |\gamma| + |\delta| = |k|.$$

Thus we can transform k to $k + \alpha'[A_t] + \alpha'[B_t]$ obtaining

$$k = e^i[A_t] + \beta[B_t] + \delta[D_t] + \gamma[C_t]$$

for some new vector $\beta \in \mathbb{F}_2^{m_t}$. Define $\theta = \beta + e^i$ so that

$$k = e^i[A_t] + e^i[B_t] + \theta[B_t] + \delta[D_t] + \gamma[C_t]. \quad (103)$$

Consider first the case when $\theta = \bar{0}$. Since k has even overlap with the stabilizer β_t^j and so does $e^i[A_t] + e^i[B_t]$, we conclude that $\delta[D_t]$ has even overlap with the gauge generator g_t^j for any j . This is possible only if $\delta = \bar{0}$ or $\delta = \bar{1}$. If $\delta = \bar{0}$ then k already has the desired form Eq. (102). If $\delta = \bar{1}_W$ then $k + g_t^t$ has the desired form and $|k + g_t^t| \leq |k|$.

Consider now the case $\theta \neq \bar{0}$. Since k has even overlap with the stabilizers β_t^j and so does $e^i[A_t] + e^i[B_t]$, we conclude that $\delta[D_t]$ has even (odd) overlap with a generator g_t^j iff θ has even (odd) overlap with the special face b^j , see Fig. 8. Let $\epsilon(\theta) \equiv |\theta| \pmod{2}$ be the total parity of θ . Let $\sigma(\theta)$ be the set of faces of Λ_t that have odd overlap with θ . The above shows that

$$\sigma(\theta) \subseteq \{b^1, b^2, \dots, b^{t-1}\}. \quad (104)$$

Note that

$$|\sigma(\theta)| = 0 \pmod{2} \quad (105)$$

since $\delta \in \mathcal{E}$, see Eq. (101). We claim that one can choose $\theta^* \subseteq \Lambda_t$ such that

$$|\theta^*| \leq |\theta|, \quad \sigma(\theta^*) = \sigma(\theta), \quad \epsilon(\theta^*) = \epsilon(\theta), \quad \text{and} \quad \text{supp}(\theta^*) \subseteq \{u^1, u^2, \dots, u^{2t+1}\}. \quad (106)$$

Recall that $u^1, u^2, \dots, u^{2t+1}$ are the sites of Λ_t located on the boundary facing Λ_{t-1} , see Fig. 7. Indeed, it is straightforward to choose some θ^* that satisfies all above conditions except for the first one. However, the property that θ^* is supported on the boundary $\omega \equiv \{u^1, u^2, \dots, u^{2t+1}\}$ implies that its weight cannot be decreased by adding faces of the lattice Λ_t . Indeed, the boundary ω is a minimum weight logical operator of the color code. This implies $|\omega + f| \geq |\omega|$ for any stabilizer $f \in \mathcal{S}_t$. Equivalently, $|f \setminus \omega| \geq |f \cap \omega|$. This implies

$$|f + \theta^*| = |f \setminus \omega| + |(f \cap \omega) + \theta^*| \geq |f \cap \omega| + |(f \cap \omega) + \theta^*| \geq |\theta^*|.$$

Finally, we note that $\sigma(\theta^*)$ and $\epsilon(\theta^*)$ fix θ^* modulo stabilizers $f \in \mathcal{S}_t$. This proves that we can satisfy all conditions in Eq. (106).

Note that $\theta[B_t] + \theta^*[B_t] \in \mathcal{U}_t$ since $\theta + \theta^* \in \mathcal{S}_t$. A gauge transformation $k \rightarrow k + \theta[B_t] + \theta^*[B_t]$ can potentially *increase* the weight of k if $i \in \theta$ but $i \notin \theta^*$. However, the weight can increase at most by two. We will “borrow” two units of weight keeping in mind that at least one of the subsequent gauge transformations has to *decrease* the weight of k at least by two, so that we maintain a zero weight balance. Transforming k to $k + \theta[B_t] + \theta^*[B_t]$ we obtain

$$k = e^i[A_t] + e^i[B_t] + \theta^*[B_t] + \delta[D_t] + \gamma[C_t]. \quad (107)$$

We have to two consider two cases.

Case 1: $\theta^* \in \mathcal{E}$. Then $u^1 \notin \theta^*$ and $u^{2t+1} \notin \theta^*$, so that θ^* consists of disjoint paths connecting consecutive pairs of faces in $\sigma(\theta^*)$. Consider any such path

$$\pi = u^{2i+1} + u^{2i+2} + \dots + u^{2m-1} + u^{2m} \subseteq \theta^*$$

that creates a pair of syndromes at faces b^i and b^m for some $i < m$. An example of such path with $i = 1$ and $m = 4$ is shown on Fig. 9. As we argued above, $\delta[D_t]$ must have odd overlap with g_r^i and g_r^m . Applying, if necessary, gauge transformations $k \rightarrow k + g_r^i$ and $k \rightarrow k + g_r^m$ we can assume that $w^{2i+1} \in \delta$ and $w^{2m} \in \delta$. Then a gauge transformation

$$k \rightarrow k + \sum_{p=i+1}^m h_t^p + \sum_{p=i+1}^{m-1} g_t^p$$

cleans k out of all qubits $\pi[B_t]$, qubits $(w^{2i+1} + w^{2m})[D_t]$, and potentially adds weight at $|\pi|$ qubits

$$(v^{2i+1} + v^{2i+2} + \dots + v^{2m-1} + v^{2m})[A_{t-1}]$$

Overall, the weight decreases at least by two, see Fig. 9.

Case 2: $\theta^* \in \mathcal{O}$. Then $u^1 \in \theta^*$ and $u^{2t+1} \in \theta^*$, so that θ^* consists of a path connecting the leftmost face in $\sigma(\theta^*)$ to the site u^{2t+1} , a path connecting the rightmost face in $\sigma(\theta^*)$ to the site u^1 , and, possibly, disjoint paths connecting consecutive pairs of faces in $\sigma(\theta^*)$, see Fig. 10. The latter can be cleaned out in the same fashion as in Case (1), so below we focus on the former. Let b^i be the rightmost face in $\sigma(\theta^*)$. Then θ^* contains a path

$$\pi_{right} = u^1 + u^2 + \dots + u^{2i-1} + u^{2i}.$$

Let b^m be the leftmost face in $\gamma(\theta^*)$. Then θ^* contains a path

$$\pi_{left} = u^{2m+1} + u^{2m} + \dots + u^{2t} + u^{2t+1}.$$

As we argued above, $\delta[D_t]$ must have odd overlap with g_t^i and g_t^m . Applying, if necessary, gauge transformations $k \rightarrow k + g_t^i$ and $k \rightarrow k + g_t^m$ we can assume that $w^{2i} \in \delta$ and $w^{2m+1} \in \delta$. Then a gauge transformation

$$k \rightarrow k + \sum_{p=1}^i h_t^p + \sum_{p=m+1}^{t-1} h_t^p + \sum_{p=1}^{i-1} g_t^p + \sum_{p=m+1}^t g_t^p$$

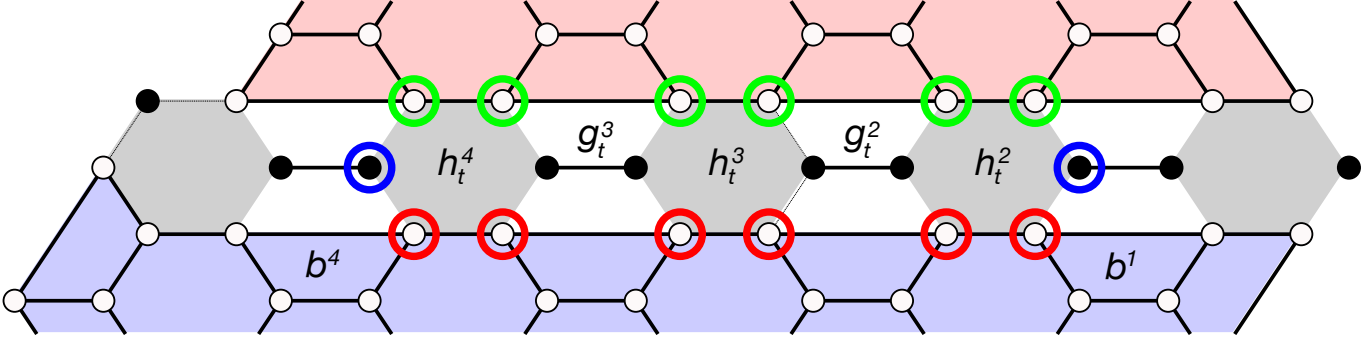


Figure 9: Example of a vector k defined in Eq. (107) such that $\theta^* \in \mathcal{E}$ creates a pair of syndromes at faces b^1 and b^4 . Sites of θ^* are indicated by red circles. In order to have zero syndrome for stabilizers β_t^1 and β_t^4 , the support of k must also include sites w^3 and w^8 (possibly, after a gauge transformation $k \rightarrow k + g_t^1$ and $k \rightarrow k + g_t^4$). The sites w^3 and w^8 are indicated by blue circles. A gauge transformation $k \rightarrow k + h_t^2 + h_t^3 + h_t^4 + g_t^2 + g_t^3$ cleans out k from all qubits indicated by blue and red circles, potentially adding weight to qubits indicated by green circles. Overall, the weight of k decreases at least by two. Here $t = 5$.

cleans k out of all qubits of $(\pi_{left} + \pi_{right})[B_t]$, qubits $(w^{2i} + w^{2m+1})[D_t]$, and potentially adds weight at $|\pi_{right}|$ qubits $(v^1 + \dots + v^{2i})[A_{t-1}]$ and $|\pi_{left}| - 2$ qubits $(v^{2m+1} + \dots + v^{2t-1})[A_{t-1}]$. Overall, the weight decreases at least by four, see Fig. 10. In both cases, we transform k to the desired form and the weight decreases at least by two. \square

The final weight reduction step is to transform the long-range generators g_r^r into a local form. We shall use a coding theory analogue of the subdivision gadget used to simulate long-range spin interactions by short-range ones [26]. Consider an arbitrary subspace $\mathcal{U} \subseteq \mathcal{E}^n$ such that $\mathcal{U} \subseteq \dot{\mathcal{U}}$ and n is odd. It defines a CSS code with a gauge group $\text{CSS}(\dot{\mathcal{U}}, \dot{\mathcal{U}})$ and a stabilizer group $\text{CSS}(\mathcal{U}, \mathcal{U})$. Note that $\mathcal{U} \subseteq \dot{\mathcal{U}}$ implies that \mathcal{U} is self-orthogonal, so that the stabilizer group is abelian and the code is well-defined. Suppose $\dot{\mathcal{U}}$ contains a weight-two vector supported on the first two qubits, $e^1 + e^2 \in \dot{\mathcal{U}}$. We envision a scenario when qubits 1 and 2 occupy two remote lattice locations (for example sites w^1 and w^{2t} in the above construction), such that $e^1 + e^2$ is not spatially local. Let us add two ancillary qubits labeled a and b . We envision that all vectors $e^1 + e^a$, $e^a + e^b$, and $e^b + e^2$ are spatially local (or, at least, more local compared with $e^1 + e^2$). Define a subspace $\mathcal{V} \subseteq \mathcal{E}_2^{n+2}$ such that

$$\dot{\mathcal{V}} = \langle e^1 + e^a, e^a + e^b, e^b + e^2 \rangle + \dot{\mathcal{U}}. \quad (108)$$

Here it is understood that vectors of $\dot{\mathcal{U}}$ are extended to the ancillary qubits by zeroes. Using analogues of Lemmas 5,6 one can easily show that \mathcal{V} is self-orthogonal, so that \mathcal{V} defines an abelian stabilizer group $\text{CSS}(\mathcal{V}, \mathcal{V})$. Below we prove that the codes $\text{CSS}(\mathcal{U}, \mathcal{U})$ and $\text{CSS}(\mathcal{V}, \mathcal{V})$ have the same distance and the same transversality properties.

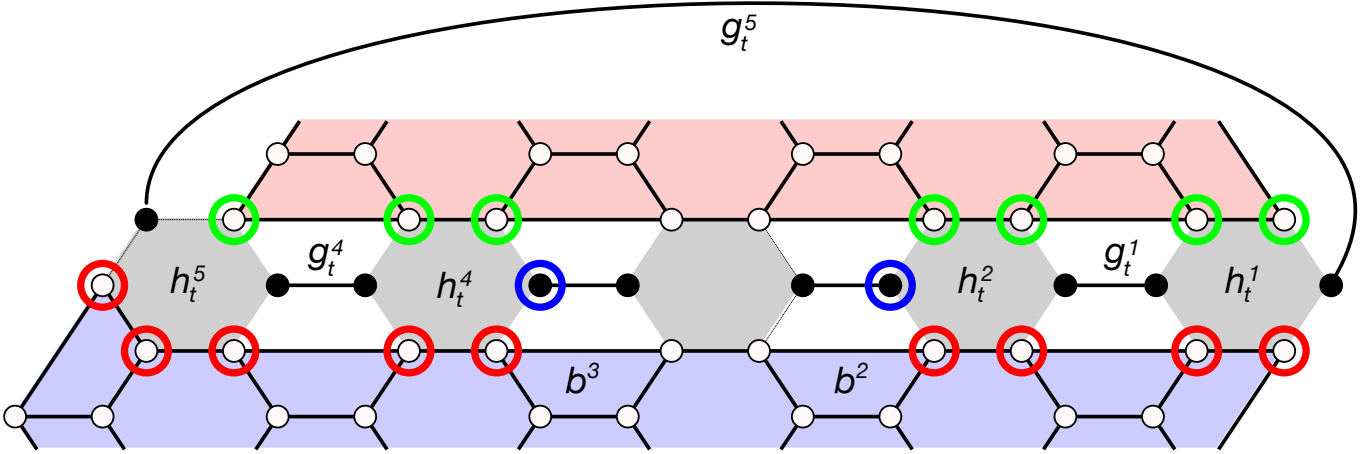


Figure 10: Example of a vector k defined in Eq. (107) such that $\theta^* \in \mathcal{O}$ creates a pair of syndromes at faces b^2 and b^3 . Sites of θ^* are indicated by red circles. In order to have zero syndrome for stabilizers β_t^2 and β_t^3 , the support of k must also include sites w^4 and w^7 (possibly, after a gauge transformation $k \rightarrow k + g_t^2$ and $k \rightarrow k + g_t^3$). The sites w^4 and w^7 are indicated by blue circles. A gauge transformation $k \rightarrow k + h_t^1 + h_t^2 + h_t^4 + h_t^5 + g_t^1 + g_t^4 + g_t^5$ cleans out k from all qubits indicated by blue and red circles, potentially adding weight to qubits indicated by green circles. Overall, the weight of k decreases at least by four. Here $t = 5$.

Lemma 9 (Subdivision gadget). *Consider the subspaces \mathcal{U} and \mathcal{V} as above. Suppose $d(\mathcal{U}) \geq 3$. Then $d(\mathcal{V}) = d(\mathcal{U})$. Furthermore, if \mathcal{U} is triply (doubly) even with respect to some subsets $M^\pm \subseteq [n]$ then \mathcal{V} is triply (doubly) even with respect to the same subsets.*

Proof. Let $\dot{\mathcal{U}}_{12}$ and \mathcal{U}_{12} be the subspaces including all vectors $g \in \dot{\mathcal{U}}$ and $g \in \mathcal{U}$ respectively such that $g_1 = g_2 = 0$, that is, g does not include qubits 1 and 2. By assumption, $e^1 + e^2 \in \dot{\mathcal{U}}$ and thus $f_1 = f_2$ for any $f \in \mathcal{U}$ since f must have even overlap with any element of $\dot{\mathcal{U}}$. There must be at least one vector $f \in \mathcal{U}$ such that $f_1 = f_2 = 1$ since otherwise $d(\mathcal{U}) = 1$. Thus \mathcal{U} can be represented as

$$\mathcal{U} = \langle e^1 + e^2 + g \rangle + \mathcal{U}_{12} \quad \text{for some } g \in \dot{\mathcal{U}}_{12}. \quad (109)$$

We claim that

$$\mathcal{V} = \langle h \rangle + \mathcal{U}_{12}, \quad \text{where } h \equiv e^1 + e^a + e^b + e^2 + g. \quad (110)$$

Let us first prove the inclusion \supseteq in Eq. (110). We have $h \in \dot{\mathcal{U}}^\perp$ since $e^1 + e^2 + g \in \mathcal{U} \subseteq \dot{\mathcal{U}}^\perp$ and $e^a + e^b \in \dot{\mathcal{U}}^\perp$ since no vector in $\dot{\mathcal{U}}$ includes a or b . Taking into account Eq. (108) one gets $h \in \dot{\mathcal{V}}^\perp$ and thus $h \in \mathcal{V}$. The inclusion $\mathcal{U}_{12} \subseteq \mathcal{V}$ follows trivially from the definitions. Next let us prove the inclusion \subseteq in Eq. (110). Consider any vector $k \in \mathcal{V}$. We note that $k_1 = k_a = k_b = k_2$ since k must have even overlap with any vector in $\dot{\mathcal{V}}$. Replacing, if necessary, k by $k + h$ we can assume that $k_1 = k_a = k_b = k_2 = 0$. Since $\dot{\mathcal{U}} \subseteq \dot{\mathcal{V}}$ we infer that $k \in \dot{\mathcal{U}}^\perp$. Taking into account that k has even weight one gets $k \in \ddot{\mathcal{U}} = \mathcal{U}$, that is, $k \in \mathcal{U}_{12}$. We have proved Eq. (110).

Suppose $f \in \mathcal{V}^\perp \cap \mathcal{O}$ is a minimum weight vector such that $|f| = d(\mathcal{V})$. Then f includes at most one of the qubits $1, a, b, 2$ since otherwise we would be able to reduce the weight of f by a gauge transformation $f \leftarrow f + f'$, where f' is contained in the first term in Eq. (108). Without loss of generality $f_a = f_b = f_2 = 0$. From Eq. (110) we infer that $h^\top f = 0$ and $f \in \mathcal{U}_{12}^\perp$. Since $f_a = f_b = 0$, this implies that f is orthogonal to $e^1 + e^2 + g$ and thus $f \in \mathcal{U}^\perp$, see Eq. (109). This shows that $f \in \mathcal{U}^\perp \cap \mathcal{O}$, that is, $d(\mathcal{V}) = |f| \geq d(\mathcal{U})$. The opposite inequality, $d(\mathcal{V}) \leq d(\mathcal{U})$, is obvious since extending any vector $f \in \mathcal{U}^\perp \cap \mathcal{O}$ by zeroes to qubits a and b gives a vector $f \in \mathcal{V}^\perp \cap \mathcal{O}$. The last statement of the lemma follows from the fact that \mathcal{U} and \mathcal{V} have the same restriction on any subset $M^\pm \subseteq [n]$, see Eq. (110). \square

It remains to apply the subdivision gadget to the long-range gauge generators $g_r^r = (w^1 + w^{2r})[D_r]$, where $r = 2, \dots, t$ (note that g_1^1 is already spatially local). Let us add a second qubit at each site w^i of the region D_r , except for w^1 and w^{2r} . We shall denote these extra qubits as $\bar{w}^2, \dots, \bar{w}^{2r-1}$ such that $D_r = \{w^1, w^2, \dots, w^{2r}, \bar{w}^2, \dots, \bar{w}^{2r-1}\}$. Qubits w^i, \bar{w}^i share the same site of the lattice. The total number of qubits becomes

$$K_t = N_t + \sum_{r=2}^t (2r - 2) = 2t^3 + 8t^2 + 6t + 1.$$

Define a subspace $\mathcal{V}_t \subseteq \mathcal{E}_2^{K_t}$ such that

$$\dot{\mathcal{V}}_t = \dot{\mathcal{U}}_t + \sum_{r=2}^t \langle (w^1 + \bar{w}^2)[D_r] \rangle + \langle (\bar{w}^{2r-1} + w^{2r})[D_r] \rangle + \sum_{i=2}^{2r-2} \langle (\bar{w}^i + \bar{w}^{i+1})[D_r] \rangle. \quad (111)$$

Here it is understood that vectors of $\dot{\mathcal{U}}_t$ are extended to the added qubits by zeroes. Note that all generators of $\dot{\mathcal{V}}_t$ are spatially local since the long-range generator g_r^r can be decomposed as

$$g_r^r = w^1 + w^{2r} = (w_1 + \bar{w}_2) + (\bar{w}_2 + \bar{w}_3) + \dots + (\bar{w}_{2r-1} + w_{2r}), \quad (112)$$

where each term has support on a single face of the lattice. Here we omitted $[D_r]$ to simplify notations. We shall regard \mathcal{V}_t as an extended version of \mathcal{U}_t . Similarly, define a subspace $\mathcal{F}_t \subseteq \mathcal{E}_2^{K_t}$ such that

$$\dot{\mathcal{F}}_t = \dot{\mathcal{D}}_t + \sum_{r=2}^t \langle (w^1 + \bar{w}^2)[D_r] \rangle + \langle (\bar{w}^{2r-1} + w^{2r})[D_r] \rangle + \sum_{i=2}^{2r-2} \langle (\bar{w}^i + \bar{w}^{i+1})[D_r] \rangle. \quad (113)$$

We shall regard \mathcal{F}_t as an extended version of \mathcal{D}_t . Note that all generators of $\dot{\mathcal{F}}_t$ are spatially local. Using Eq. (95) and analogues of Lemmas 5,6 one can easily show that

$$\mathcal{V}_t \subseteq \mathcal{F}_t \subseteq \dot{\mathcal{F}}_t \subseteq \dot{\mathcal{V}}_t. \quad (114)$$

We are now ready to define the final version of the doubled color codes, see Table 4, that satisfy all the properties announced in Section 8 (up to relabeling of the subspaces $\mathcal{C}_t, \mathcal{T}_t$ into $\mathcal{F}_t, \mathcal{V}_t$). Combining

Eq. (7) and Eq. (114) one can see that the distance of any code defined in Table 4 is lower bounded by $d(\mathcal{V}_t)$. A recursive application of the subdivision gadget lemma shows that $d(\mathcal{V}_t) = d(\mathcal{U}_t) = 2t + 1$. Furthermore, \mathcal{V}_t is triply-even with respect to the same subsets as \mathcal{U}_t and \mathcal{F}_t is doubly even with respect to the same subsets as \mathcal{D}_t . Thus the final C and T codes have transversal Clifford gates and the T -gate respectively. Let us describe gauge generators of the final C -code. From Eq. (112)

	Transversal gates	Stabilizer group	Gauge group
C -code	Clifford group	$\text{CSS}(\mathcal{F}_t, \mathcal{F}_t)$	$\text{CSS}(\dot{\mathcal{F}}_t, \dot{\mathcal{F}}_t)$
T -code	T gate	$\text{CSS}(\mathcal{V}_t, \dot{\mathcal{V}}_t)$	$\text{CSS}(\mathcal{V}_t, \dot{\mathcal{V}}_t)$
Base code		$\text{CSS}(\mathcal{V}_t, \mathcal{F}_t)$	$\text{CSS}(\dot{\mathcal{F}}_t, \dot{\mathcal{V}}_t)$

Table 4: Final version of the doubled color codes. All gauge generators of the C -code are spatially local. The T -code can be obtained from the C -code by measuring syndromes of edge-type stabilizers. The base code is defined such that its stabilizer group is the intersection of all other stabilizer groups.

we infer that the long-range generators g_r^r can be removed from the generating set. Thus the final C -code has only face-type gauge generators, the additional generators $g_r^1, \dots, g_r^{r-1}, h_r^1, \dots, h_r^r$, and the additional generators that appear in Eq. (113). All these generators are spatially local. The same arguments as above show that a restriction of the final C -code onto the region A_t coincides with the regular color code $\text{CSS}(\mathcal{S}_t, \mathcal{S}_t)$. As before, the final T -code is obtained from the extended C -code by adding edge-type stabilizer generators.

Finally, let us point out that the gauge generator $\omega_{1,0} \in \dot{\mathcal{T}}_t$ is already spatially local, so that we do not have to apply the weight reduction steps to $\omega_{1,0}$. Thus the total number of physical qubits can be reduced from K_t to $K_t - 2 = 2t^3 + 8t^2 + 6t - 1$.

Acknowledgments

SB thanks Andrew Landahl for fruitful discussions and helpful suggestions at the early stages of this project. SB acknowledges NSF grant PHY-1415461.

References

- [1] R. Barends, J. Kelly, A. Megrant, A. Veitia, D. Sank, E. Jeffrey, T.C. White, J. Mutus, A. Fowler, B. Campbell, et al. Superconducting quantum circuits at the surface code threshold for fault tolerance. *Nature*, 508(7497):500–503, 2014.
- [2] J. Kelly, R. Barends, A. Fowler, A. Megrant, E. Jeffrey, T.C. White, D. Sank, J. Mutus, B. Campbell, Y. Chen, et al. State preservation by repetitive error detection in a superconducting quantum circuit. *Nature*, 519(7541):66–69, 2015.

- [3] A. Córcoles, E. Magesan, S. Srinivasan, A. Cross, M. Steffen, J. Gambetta, and J. Chow. Demonstration of a quantum error detection code using a square lattice of four superconducting qubits. *Nature Communications*, 6:6979, 2015.
- [4] E. Dennis, A. Kitaev, A. Landahl, and J. Preskill. Topological quantum memory. *J. of Math. Phys.*, 43(9):4452–4505, 2002.
- [5] R. Raussendorf and J. Harrington. Fault-tolerant quantum computation with high threshold in two dimensions. *Phys. Rev. Lett.*, 98(19):190504, 2007.
- [6] A. Fowler, A. Stephens, and P. Groszkowski. High-threshold universal quantum computation on the surface code. *Phys. Rev. A*, 80(5):052312, 2009.
- [7] C. Jones. Logic synthesis for fault-tolerant quantum computers. *preprint arXiv:1310.7290*, 2013.
- [8] A. Fowler, S. Devitt, and C. Jones. Surface code implementation of block code state distillation. *Scientific Reports*, 3:1939, 2013.
- [9] B. Eastin and E. Knill. Restrictions on transversal encoded quantum gate sets. *Phys. Rev. Lett.*, 102(11):110502, 2009.
- [10] S. Bravyi and R. König. Classification of topologically protected gates for local stabilizer codes. *Phys. Rev. Lett.*, 110(17):170503, 2013.
- [11] F. Pastawski and B. Yoshida. Fault-tolerant logical gates in quantum error-correcting codes. *Phys. Rev. A*, 91(1):012305, 2015.
- [12] M. Beverland, R. König, F. Pastawski, J. Preskill, and S. Sijher. Protected gates for topological quantum field theories. *preprint arXiv:1409.3898*, 2014.
- [13] A. Paetznick and B. Reichardt. Universal fault-tolerant quantum computation with only transversal gates and error correction. *Phys. Rev. Lett.*, 111(9):090505, 2013.
- [14] J. Anderson, G. Duclos-Cianci, and D. Poulin. Fault-tolerant conversion between the Steane and Reed-Muller quantum codes. *Phys. Rev. Lett.*, 113(8):080501, 2014.
- [15] E. Knill, D. Leibfried, R. Reichle, J. Britton, R.B. Blakestad, J.D. Jost, C. Langer, R. Ozeri, S. Seidelin, and D.J. Wineland. Randomized benchmarking of quantum gates. *Phys. Rev. A*, 77(1):012307, 2008.
- [16] J. Chow, J. Gambetta, L. Tornberg, J. Koch, L. Bishop, A. Houck, B.R. Johnson, L. Frunzio, S. Girvin, and R. Schoelkopf. Randomized benchmarking and process tomography for gate errors in a solid-state qubit. *Phys. Rev. Lett.*, 102(9):090502, 2009.
- [17] B.J. Brown, H. N. Naomi, and D.E. Browne. Fault-tolerant error correction with the gauge color code. *preprint arXiv:1503.08217*, 2015.

- [18] H. Bombin. Gauge color codes: optimal transversal gates and gauge fixing in topological stabilizer codes. *New J. Phys.*, 17(8):083002, 2015.
- [19] C. Wang, J. Harrington, and J. Preskill. Confinement-Higgs transition in a disordered gauge theory and the accuracy threshold for quantum memory. *Ann. of Phys.*, 303(1):31–58, 2003.
- [20] K. Betsumiya and A. Munemasa. On triply even binary codes. *preprint arXiv:1012.4134*, 2010.
- [21] A. R. Calderbank and P. W. Shor. Good quantum error-correcting codes exist. *Phys. Rev. A*, 54(2):1098, 1996.
- [22] A.M. Steane. Multiple particle interference and quantum error correction. *Proc. Roy. Soc. Lond. A*, 452:2551–2577, 1996.
- [23] H. Bombin and M. A. Martin-Delgado. Topological quantum distillation. *Phys. Rev. Lett.*, 97(18):180501, 2006.
- [24] A. Kubica and M. Beverland. Universal transversal gates with color codes: a simplified approach. *Phys. Rev. A*, 91(3):032330, 2015.
- [25] A. Kitaev. Fault-tolerant quantum computation by anyons. *Ann. of Phys.*, 303(1):2–30, 2003.
- [26] R. Oliveira and B. Terhal. The complexity of quantum spin systems on a two-dimensional square lattice. *Quant. Inf. and Comp.*, 8(10):900–924, 2008.
- [27] S. Bravyi and J. Haah. Magic-state distillation with low overhead. *Phys. Rev. A*, 86(5):052329, 2012.
- [28] A. Landahl and C. Ryan-Anderson. Quantum computing by color-code lattice surgery. *preprint arXiv:1407.5103*, 2014.
- [29] V. Kliuchnikov, D. Maslov, and M. Mosca. Fast and efficient exact synthesis of single-qubit unitaries generated by Clifford and T gates. *Quant. Inf. and Comp.*, 13(7-8):607–630, 2013.
- [30] P. Selinger. Efficient Clifford+T approximation of single-qubit operators. *Quant. Inf. and Comp.*, 15(1-2):159–180, 2015.